Journal of South American Earth Sciences 97 (2020) 102423

Contents lists available at ScienceDirect

Journal of South American Earth Sciences

journal homepage: www.elsevier.com/locate/jsames

Geology, petrology and geochronology of sierra Valle Fértil - La Huerta batholith: Implications for the construction of a middle-crust magmatic-arc section

Giuliano Camilletti[a,*], Juan Otamendi[a], Alina Tibaldi[a], Eber Cristofolini[a], Mathieu Leisen[b], Rurik Romero[b], Fernando Barra[b], Paula Armas[a], Matías Barzola[a]

[a] CONICET, Departamento de Geología, Universidad Nacional de Río Cuarto, Campus Universitario, X5804BYA, Río Cuarto, Argentina
[b] Departamento de Geología, Universidad de Chile, Plaza Ercilla 803, Santiago, Chile

ARTICLE INFO

Keywords:
Ordovician
Gondwana
Famatinian arc
Igneous petrology
Magmatic system

ABSTRACT

The Valle Fértil-La Huerta batholith is a differentially tilted, compositionally stacked, calc-alkaline plutonic sequence in the central Famatinian arc of Argentina. It consists of two major lithologic units: these are (1) an intermediate unit largely dominated by amphibole- and biotite-bearing tonalites but encompassing from gabbro to leucogranite; and (2) an overlying silicic unit that shows the same petrological diversity as the intermediate unit, but granodiorite and monzogranite are its prevailing lithologies. The silicic unit is separated into four subunits using lithological changes at regional mapping scale. All the boundaries are gradational among lithologic units and subunits. The internal fabric along the entire batholith is either magmatic or submagmatic and it was developed during the arc formation. The original magmatic foliation is north–south striking and steeply-dipping. The magmatic foliation crosses over and transposes the gradational contacts among lithologic units. Petrological architecture, structural geology, geobarometric estimates and geochronology show that the entire batholith is a comagmatic system exposing more than 13 km of a middle arc crust. Crystallization-fractionation models computed using whole rock and mineral chemistry account for the mineralogy of plutonic rocks and coincide with the results of experimental petrology. Mass-balanced modeling predicts that the unexposed cumulate roots of the Famatinian arc should have been about 1.3 times larger than the intermediate and silicic plutonic batholith. However, the mass of calculated cumulate would diminish significantly if a portion of the host metasedimentary material were consumed in constructing the batholith. The batholith grew progressing upward from the lowest levels and acquired a stratified compositional organization. The driving mechanism was continuous influxes of mantle-derived mafic magmas that made up the lower crust, caused crustal-level melting and magma mixing, and formed intermediate – silicic rocks at increasingly shallower depths.

1. Introduction

The unique petrologic expression of arc magmatism is the result of subduction zone geodynamics (Ringwood, 1974; McCulloch and Gamble, 1991). Prevailing scientific thought emphasizes percolation of slab-derived partial melts and hydrous fluids from the oceanic crust into the corner-flowing mantle wedge as the decisive mechanisms for subduction zone magmatism (Davies and Stevenson, 1992). Within the overriding plate, as De Bari (1997) showed, the chemistry of subduction-related primitive magmas is broadly the same in continental and oceanic arcs, so drawing attention to the role of intra-crustal differentiation. The construction of a continuous arc section from the petrological Moho to the volcanic plumbing system significantly depicts the petrological diversity of a transcrustal magmatic system (Bachmann and Bergantz, 2008; Cashman et al., 2017). Reconstructing magmatic processes from an arc where all levels of it are exposed is a powerful mean for understanding the processes operating in arc magmatic systems that are responsible for: (1) the construction of a transcrustal magmatic column, and (2) the driving force behind fiery eruptions (Putirka, 2017). The task requires the combination of field studies with geochemistry, geochronology and geobarometry to achieve full integration of the petrological processes from the mantle cumulates to subvolcanic products (Jagoutz and Kelemen, 2015; Cashman et al., 2017). This is what is known, but what is still not fully understood is

* Corresponding author.
E-mail address: giuliano.camilletti026@gmail.com (G. Camilletti).

https://doi.org/10.1016/j.jsames.2019.102423
Received 11 February 2019; Received in revised form 14 November 2019; Accepted 14 November 2019
Available online 20 November 2019

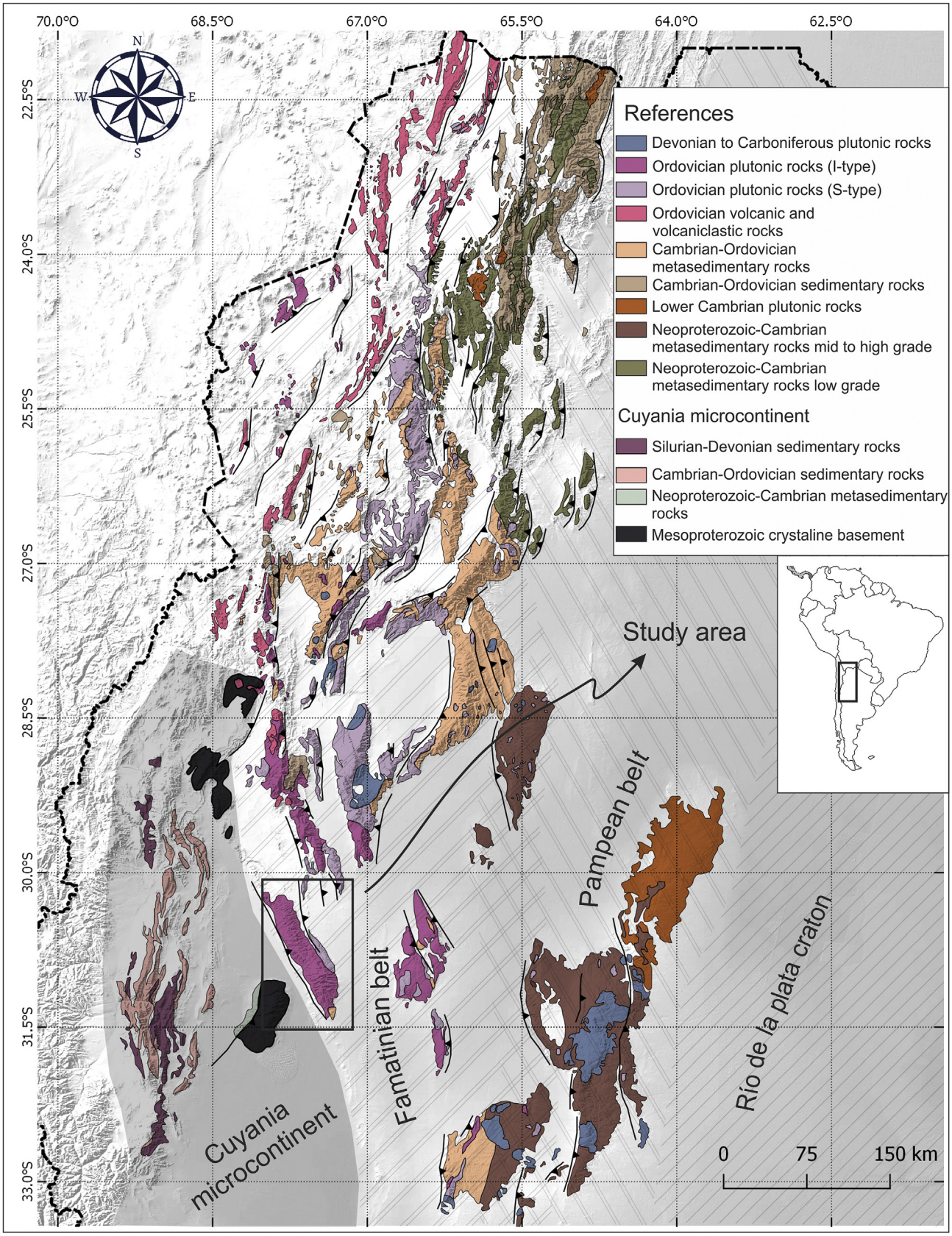

Fig. 1. Simplified geological map showing the distribution of rocks formed within the Famatinian magmatic arc. The map also includes the lithostratigraphic units that are important to construct the geological setting of the Famatinian arc. Inset shows the location map of the studied area in Argentina.

exactly how and where magmas differentiate from their primitive chemistry in the deep crust to the dominant intermediate and silicic middle and upper batholithic crust (Bateman and Dodge, 1970; Collins, 1996; Jagoutz, 2010; among others). Certainly, a complete view of petrological differentiation on transcrustal magmatism systems require a natural window into the process, however, most of the Phanerozoic subduction-related Cordilleran-style batholiths only allow observing their shallow parts (Paterson and Ducea, 2015). There is a need for deeply exposed natural examples to constraint what are otherwise inferences from petrological and geochemical reasoning.

The sierra Valle Fértil – La Huerta provides a singular opportunity to study a batholith in cross-section, it conforms a tilted and relatively undeformed section of the middle to upper crust of the Famatinian arc (Fig. 1). The presence of metasedimentary rocks within the entire batholith allows retrieving the crystallization paleodepth of plutonic rocks hosting each supracrustal screen. In addition to this, the lack of major tectonic breaks permits rationally restoring the original stacking of the petrological column. These are two geological qualities making the sierra Valle Fértil – La Huerta (hereafter VFLH) a natural laboratory for the study of structural and petrogenetic relations in a comagmatic intermediate to silicic arc crustal section.

Both the southern part and the east flank of the VFLH batholith remain almost unexplored, since previous studies comprise the Valle Fértil type section, which is an east-west cross-section located in the center of the batholith (Otamendi et al., 2012, 2009; 2017; Tibaldi et al., 2013; Walker et al., 2015; Cristofolini et al., 2014; among others). This study presents new field and structural observations, major oxide geochemistry, petrographic data, geochronology and geobarometry over a large region of the VFLH batholith that is little known (Fig. 2, zones a, b and c). These new observations and data are correlated with previous studies in a comprehensive geological map. All the new data are combined to model the construction of a middle-crust magmatic-arc section.

2. Geologic background

Below is a summary of the geologic history of the sierra Valle Fértil at 32°S, within the context of the Paleozoic geology of central and northwestern Argentina (Fig. 1).

Phase 1: After Early Cambrian Pampean Orogeny, Upper Cambrian turbidites, called Negro Peinado Formation, and its equivalents at variable crustal levels were deposited on offshore basins in the margin of West Gondwana. These sedimentary successions underwent a rapid burial to mid-crustal depths, and then they became the host units of the Early Ordovician arc (Collo et al., 2009; Ducea et al., 2010; Cristofolini et al., 2012; Mulcahy et al., 2014).

Phase 2: Intruding into the Upper Cambrian succession is a thick sequence of Early Ordovician to Middle Ordovician arc-related transcrustal magmatic system (Otamendi et al., 2017), which forms part of a continental-scale arc that extended from northern Patagonia in Argentina to Cordillera de Mérida in Venezuela (Pankhurst et al., 1998; Cawood, 2005; Chew et al., 2007; Ramos, 2018). A striking feature of the Famatinian arc is the general lack of older basement within the exposed arc crustal section; instead, the only country rocks of the Famatinian arc (even when exposed at deep crustal levels) are metasedimentary assemblages. The total crustal thickness during the magmatic peak is difficult to reconstruct. A reconstruction through thermobarometry indicates a minimum thickness of 27 km. The boundary between the crust and the lithospheric mantle is not observed. A general model for the Famatinian arc suggests a total crustal thickness of between 30 and 35 km (Tibaldi et al., 2013). Of interest here, the middle arc crust comprises a vertical exposure of ~13 km between paleodephts of 26 km–13 km.

Phase 3: Subduction-related magmatic activity in the central section of the arc (south of 27° South latitude) ended at about 465 Ma when an allochthonous terrane collided against the Gondwana margin (Thomas and Astini, 1996; Astini and Dávila, 2004; Benedetto, 2004; Ramos, 2004). After about 200 Ma of mountain building followed by orogenic collapse, the Famatinian arc plutonic crust became the basement of Carboniferous sediments (Otamendi et al., 2009; Cristofolini et al., 2014). By the Carboniferous, Gondwana's margin had migrated hundreds of kilometers outboard and established along the present-day Chile-Argentina border (Creixell et al., 2016).

Phase 4: Shallow subduction of the Nazca plate beneath South America at the latitude of this study commenced about 18 Ma ago, a process driven by the subduction of the Juan Fernández Ridge (Yáñez et al., 2001). During the past 15 Ma, the coupling between the two plates increased and the Andean deformation front migrated inland (Jordan and Allmendinger, 1986; Ramos et al., 2002). In this context, sierra Valle Fértil – La Huerta is a fault-bounded crystalline basement-cored uplift.

The sierra Valle Fértil – La Huerta is composed predominantly of Ordovician plutonic rocks and constitutes an eastward-tilted arc crust (Otamendi et al., 2009). To the west, the section is cut by the Valle Fértil lineament, a major shear zone that represents a terrain boundary (Astini and Dávila, 2004; Cristofolini et al., 2014). U–Pb zircon crystallization ages ranging from 476 to 469 Ma for all the different plutonic rocks that constitute the batholith (Pankhurst et al., 2000; Ducea et al., 2010, 2017; Castro et al., 2014; Otamendi et al., 2017; Rapela et al., 2018).

The lithologic mafic unit represents the deepest exposed crustal levels and is dominated by amphibole gabbronorite and orthopyroxene-amphibole-biotite diorite. The whole-rock composition reveals that almost all the gabbroic rocks are cumulates. Olivine-bearing layered bodies preserve the igneous features from millimeter to whole body length scales (Otamendi et al., 2010). A cross-sectional view through the sierra Valle Fértil – La Huerta suggests that a tonalite-dominated intermediate unit grew overlying the mafic unit (Tibaldi et al., 2013).

The metasedimentary rocks constitute a litho-stratigraphic unit that occurs as km-long belts interstratified among the plutonic lithological units. Furthermore, metasedimentary rocks identical to those defining the unit also appear widespread as meter-long fragments within the igneous batholith. Irrespective of the protolith, all migmatites have leucogranitic leucosomes. Some anatectic leucogranitic lens-shaped sills and dikes occur in the metasedimentary unit. Anatectic granites appear as discrete bodies in other lithological units and show field-based evidence of interaction with mafic, intermediate and silicic plutonic rocks (Walker et al., 2015).

3. Plutonic stratigraphy of the intermediate and silicic rock units

The igneous stratigraphy of the sierra Valle Fértil – La Huerta is organized using rock units (Otamendi et al., 2009). The criteria to separate the batholith into units is according to the preponderance of igneous rock associations so, the main feature of each unit comes from the dominant lithology. In general, each rock unit forms an elongated sub-meridionally trending belt. The boundaries between units are transitional. We provide a lithologic relationship for many cross-sections along the south half part and the eastern part of the batholith that are neither mapped nor sampled (Fig. 2, zones a, b and c). Furthermore, the study also addresses a correlation between the areas of the batholith studied here with the type section (Otamendi et al., 2012).

3.1. Intermediate unit

The intermediate unit is the main area of the VFLH batholith and constitutes a continuous belt along the sierra. This unit extends along the center of the sierra Valle Fértil – La Huerta and eastwards it grades into the silicic unit (Fig. 2, “b” zone). The intermediate unit is thick (ca. 20 km wide) in the south (“a” zone). Then the unit shrinks northward and is exposed as a narrow belt (ca. 10 km wide) between the mafic unit and the silicic unit in the central section of the sierra Valle Fértil – La

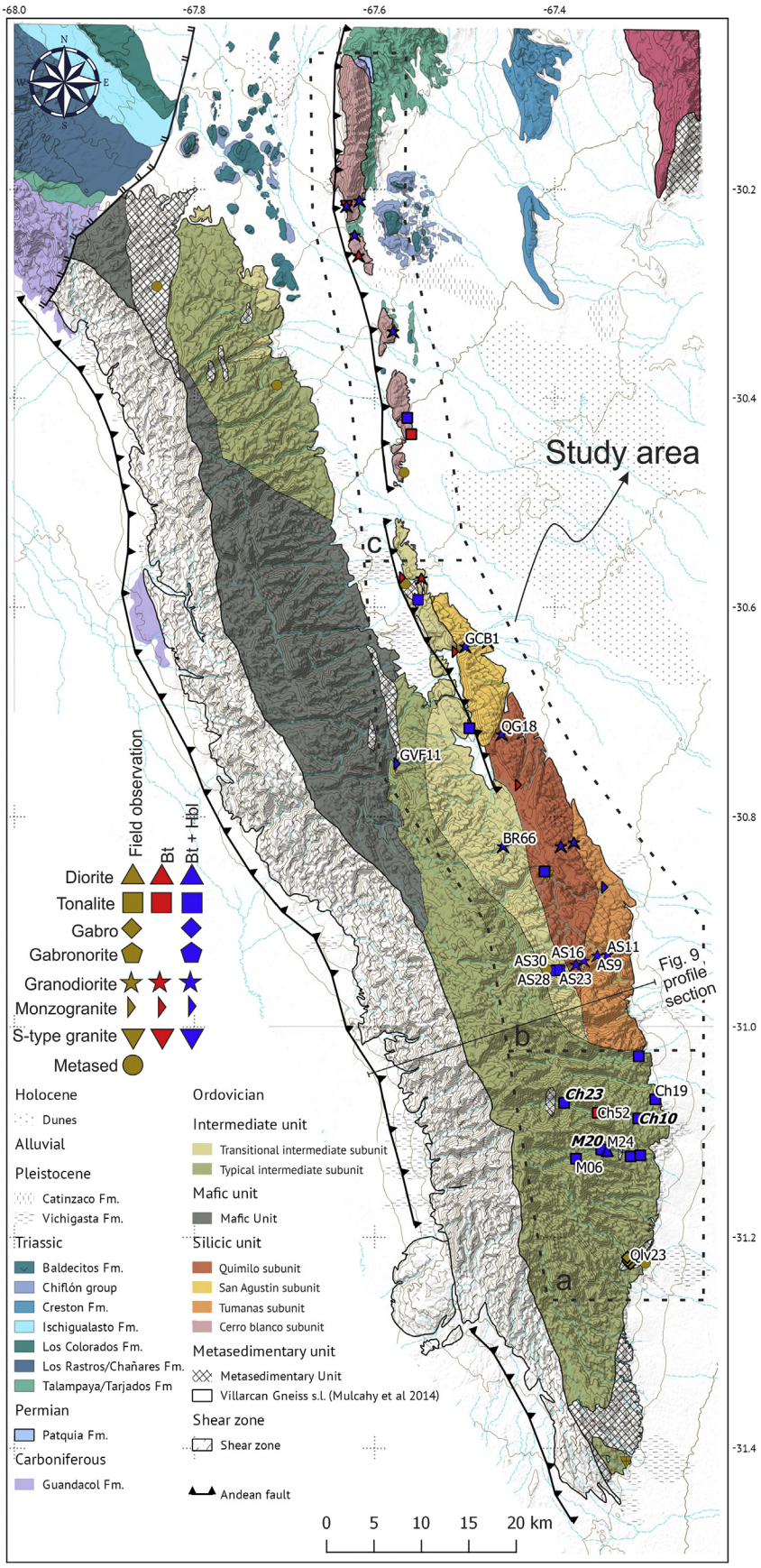

Fig. 2. Geological map of the Sierras Valle Fértil and La Huerta. The map presents the distribution of rock type with modal of amphibole and biotite that compose the plutonic batholith. All the samples in the map have whole-rock geochemistry. Labeled samples have mineral geochemistry. Samples taken to perform zircon geochronogy are shown in bold and italic case.

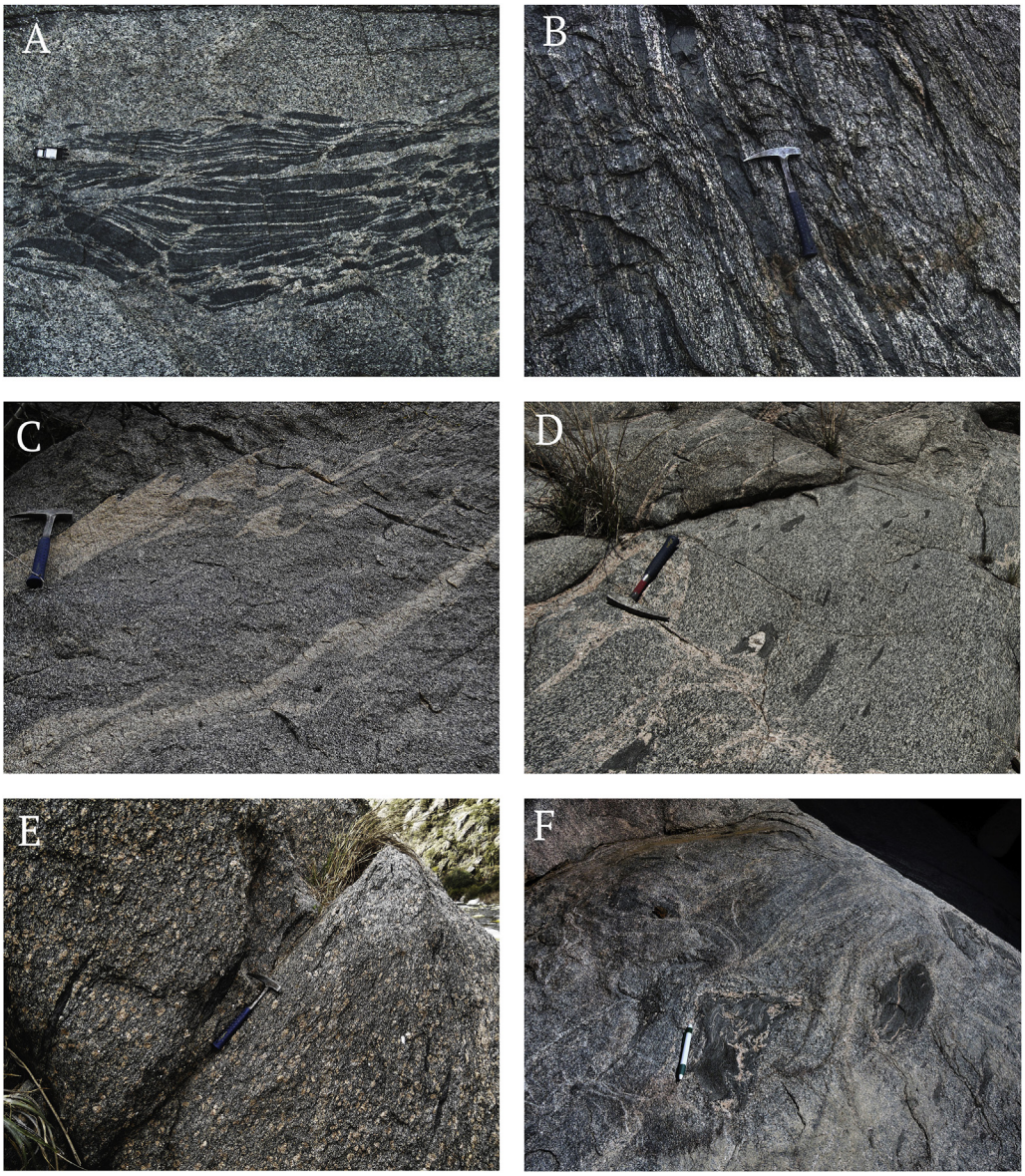

Fig. 3. (A) Field photography of typical tonalite in the intermediate subunit. A mafic syn-plutonic dike is shown partially dismembered by the magmatic flow of the tonalitic magma. (B) Interlayering of tonalites with tabular-shaped mafic inclusion representing magma pathways in the middle Famatinian arc crust. Magmatic flow of the tonalitic magma stretched and parallelized the already solid microgranular mafic rocks. (C) Magma mingling between leucogranites and tonalites that occurred in magmatic middle-crustal levels. A contrasting rheological response is shown by magmatically folded leucogranites that are wrapped by the sub-parallel magmatic foliation of the tonalite. (D) Magma mingling as flow structures where leucogranitic veins and magmatic enclaves are dispersed within tonalitic plutonic rock (E) Photography of the granodiorite that dominates Quimilo pluton showing strong mineral preferred orientation of K-feldspar megacrysts. (F) Viscous folding of magmatic sheets that do not show sub-solidus deformation at grain scale.

Huerta (Otamendi et al., 2009). The intermediate unit is divided into two subunits based on lithological diversity. The subunits are: (1) the typical intermediate subunit, and (2) the transitional intermediate subunit (Fig. 2 “a” and “b” zones).

The typical intermediate subunit consists of tonalites and quartz-diorites. These rocks are often-sheeted and show a varying degree of heterogeneities on a scale of tens of meters. The subunit rocks have a mottled aspect due to the mafic minerals forming clusters. The dominant tonalites contain synplutonic dikes, magmatic enclaves (isolated or swarm-like, Fig. 3a), and metasedimentary xenoliths.

A great majority of the typical intermediate subunit consists of tonalites. The medium-to coarse-grained equigranular tonalites contain hornblende + plagioclase + biotite ± orthopyroxene ± clinopyroxene. The tonalitic rocks exhibit limited-ranging mineralogy with the only variation being the proportion of mafic minerals. The tonalites exhibit mostly a hypidiomorphic granular texture. Plagioclase is subhedral optically unzoned and includes zircon, quartz, apatite, and oxides. Quartz is anhedral, appears filling pores, and displays undulatory extinction and an incipient grain-boundary migration. There is quartz that formed along grain boundaries and fills the intervening spaces between fractured primary plagioclase crystals. Hornblende is prevailing, though biotite is always present, orthopyroxene and clinopyroxene are rare and are replaced by hornblende.

Into the intermediate unit are locally abundant bodies of olivine gabbros, two-pyroxene gabbronorites and amphibole granodiorites. Mafic magmatic aggregates are widespread and hosted in the plutonic rocks. The aggregates occur as discrete microgranular enclaves or schlieren layering (Fig. 3b) and, at an outcrop scale, they vary widely from almost absent to tightly packed swarms. Enclaves are oblate ellipsoids, their size varies from 1 to 2 cm to > 3 m long, and their contact with the host plutonic rock is either sharp or gradational. The magmatic enclaves have hornblende-dominated mineral assemblage and a fine-to medium-grained, idiomorphic textures.

The transitional intermediate subunit is a discrete belt that is overlying the typical intermediate subunit and underlying the entire silicic unit (Tibaldi et al., 2013) (Fig. 2, “b” zone). A distinctive feature of the transitional subunit is a widespread mingling (i.e., uncompleted-magma-mixing) between tonalitic and leucogranitic rocks (Fig. 3c). Generally, mingling occurs as flow structures where leucogranitic veins or dike-like layers are dispersed within tonalitic plutonic rock (Fig. 3d).

The tonalitic rocks are the most abundant component of the mingled rocks. Thus, the intermediate rocks host the intrusive leucogranites. Tonalites are mesocratic and consist of plagioclase + hornblende + biotite + epidote ± K-feldspar ±

sphene. Plagioclase is subhedral. Quartz is interstitial. Clots of hornblende, biotite and oxides form dark mineral clusters. Hornblende is large, subhedral and usually replaced by biotite. The appearance of accessory sphene coexisting with ilmenite is a unique mineralogical singularity of the transitional subunit due to sphene is absent in tonalites from the typical intermediate subunit.

The intrusive leucogranites are felsic syenogranites that only bear scarce biotite with accessory zircon and magnetite. Leucogranitic lenses and layers are perfectly concordant with the magmatic foliation of the tonalite (Fig. 3c).

3.2. Silicic unit

Flanking along the eastern boundary and overlying the intermediate unit, the silicic unit covers a large area that extends from the central sierra Valle Fértil – La Huerta to the southern tips of the Famatina Mountains (Fig. 1).

The silicic unit consists of four subunits, from south to north; Tumanas, Quimilo, San Agustin and Cerro Blanco (Fig. 2, zones "b" and "c"). The plutonic subunits appear as a north–south belt and extend over kilometers in length. The exposed boundaries among Tumanas, Quimilo, and San Agustin are gradational and complex. Each subunit has a relative abundance of tonalites, granodiorites, monzogranites, and leucogranites. However, all the subunits show commingling among these lithologies.

The Tumanas subunit is the southern extension of the silicic unit and shows two original boundaries. The long-transitional contact between Tumanas and Quimilo subunits is defined by the absence of K-feldspar megacrysts in the former, while the essential and accessory mineralogy vary little between them. The boundary of the Tumanas subunit on its southern tip is transitional, it grades over tens of meters to the tonalites of the typical intermediate subunit. The Tumanas subunit consists of granodiorites, with subordinate presence of monzogranites and tonalites. The texture of nearly all granodiorites is hypidiomorphic granular and the common mineral assemblage is plagioclase + K-feldspar + quartz + biotite + hornblende, with epidote, sphene, apatite, zircon and oxides as accessory minerals. K-feldspar is subhedral and develops myrmekite in contact with plagioclase. Hornblende is anhedral fine-grained and form clusters with biotite, epidote, sphene, and oxides. Laminar and tabular minerals show a well-defined orientation.

The Quimilo subunit spreads over a large area among the transitional intermediate subunit, San Agustin and Tumanas silicic subunits (Fig. 2, "b" zone). The texture of the granodiorite is porphyritic, containing megacrysts of K-feldspar (< 5 cm) with inclusions of plagioclase, quartz, and biotite (Fig. 3e). The medium-grained groundmass is similar in mineralogy to a tonalite and biotite can exceed hornblende in abundance. The alignment of K-feldspar megacrysts together with the mineral preferred orientation of biotite and hornblende define a prevalent magmatic fabric.

Leucogranites appear all over the Quimilo subunit. The size of the leucogranitic bodies is variable from meter-scale lens-shaped veins to hundred-meter long dikes. They display both mingling and intrusive relations with the megacrystic granodiorite, usually subconcordant with the magmatic fabric. Dish-shaped magmatic enclaves are widespread and parallel to the preferred alignment of the magmatic minerals (Fig. 3e).

Plutonic rocks of San Agustin subunit range from granodiorites to syenogranites, with minor interspersed tonalites. The texture of the prevailing granodiorite is granular and hypidiomorphic. The mineral assemblage is plagioclase + quartz + K-feldspar + biotite ± hornblende ± epidote ± apatite ± zircon ± sphene ± oxides. Euhedral plagioclase is strongly zoned. K-feldspar is subhedral, medium-grained and with a pertitic texture. Hornblende is anhedral, medium-to fine-grained and usually rimmed by biotite. Epidote is euhedral, sometimes allanite-cored, and remarkably widespread. Sphene is normally euhedral but, corroded and less abundant than epidote. The preferred orientation of tabular-shaped euhedral plagioclase and K-feldspar defines the magmatic fabric. Within the subunit several small lens-shaped leucogranite bodies are scattered. These bodies are related to metasedimentary septa that are dispersed throughout the subunit as a block of tens of meters in length.

Mafic amphibole-rich enclaves are widespread in the San Agustin subunit, usually accumulated in pipe-like structures (Castro et al., 2008). The magmatic enclaves frequently are disaggregated and are identified as such because they consist of fine-grained biotite and amphibole clots coexisting with coarse-grained K-feldspar and quartz (Fig. 3f). The same type of amphibole-rich mafic rocks is frequent in the silicic unit as discrete bodies with sizes of up to 1 km^2 of areal extensions.

The northern Cerro Blanco subunit is a fault-bounded N– S trending belt and is either unconformably covered by Permo-Triassic continental sedimentary successions or surrounded by Quaternary alluvial fans (Fig. 2, "c" zone). Cerro Blanco subunit is the stratigraphically shallowest exposure of the VFLH batholith. This subunit mainly consists of hornblende- and biotite-bearing tonalites, but it also contains quartz-diorites, granodiorites, and sparse monzogranites. Importantly, all the boundaries among the prevailing tonalites and the subordinated lithologies are gradational and related to commingling. Tonalites have a hypidiomorphic inequigranular coarse-to medium-grained texture. They have an invariable mineral assemblage consisting of plagioclase + quartz + K-feldspar + biotite + hornblende ± sphene ± muscovite ± apatite ± epidote ± zircon ± oxides. Plagioclase is the dominant essential phase, is subhedral and has inclusions of epidote, biotite, and oxides. Quartz is anhedral and shows undulatory extinction. K-feldspar is fine-grained and forms myrmekite in contact with plagioclase. Tonalites contain pale red-brown biotite coexisting with green prismatic hornblende.

4. Structural characteristics

The data presented here is focused on analyzing the nature of the magmatic stage; however, the structural data include the solid-state high-temperature structural features that affected the original magmatic fabric.

The magmatic foliation was identified following the criteria of Paterson et al. (1989). The igneous fabric is defined by the alignment of plagioclase laths, K-feldspar megacrysts (when present), elongated hornblende prism, biotite [001] faces, and sparse ellipsoidal magmatic enclaves. The limits of enclaves with the hosting plutonic rock are variable, ranging from sharp to gradational. In the last case, plagioclase laths from the host surround and penetrate the enclave to variable degrees. The entrance of plutonic minerals into the enclave ranges from a few distributed grains inside enclaves to examples where plagioclase aggregates dominate been the enclaves partially disintegrated into the matrix. Plagioclase (xeno)crystals in the enclave exhibit preferred orientation that is also parallel to hornblende prisms. The magmatic foliation developed into the enclave is continuous with the foliation of the host plutonic rock reflecting that both enclave and host had similar effective viscosities during syn-magmatic deformation (Webber et al., 2015).

The plutonic rocks are affected by a crystal-plastic deformation characterized by subgrain development in quartz, slightly deformed twins in plagioclase and curved cleavage in biotites. The crystal-plastic deformation is aligned with and overprinting the magmatic foliation.

The magmatic foliation exhibits, all over the typical intermediate subunit, a NNW-SSE trend with steeply to moderate dipping (46°–78°) to the west (Fig. 4, "a" zone). However, close to its western limit, the magmatic and/or submagmatic foliations are overprinted by the mylonite-series fabrics that are penetrative along the western VFLH shear zone (Cristofolini et al., 2014).

Within the transitional intermediate subunit (Fig. 4, "b" zone) exists

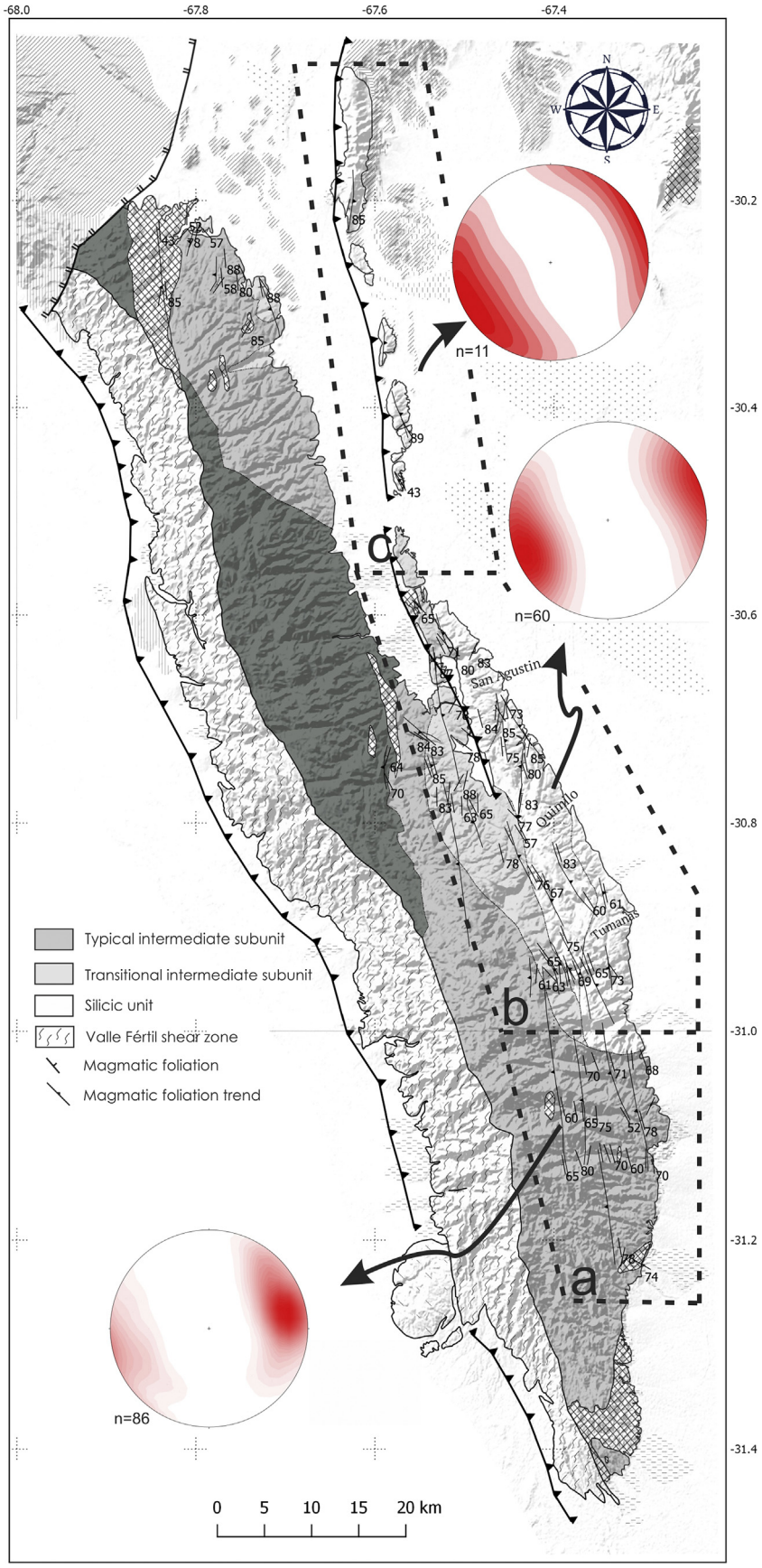

Fig. 4. Simplified geological map showing the magmatic foliation pattern in the VFLH batholith. Equal area stereoplots show densities of poles to foliation measured along the batholith.

a broad area of mingled plutonic rocks showing evidence of magmatic flow at all scales. The magmatic structures are: (1) parallel alignment of leucogranitic layers with long-shaped crystals in the hosting tonalitic rocks (Fig. 3c), (2) magmatic flow foliations wrapping around ellipsoidal mafic magmatic enclaves (Fig. 3a), and (3) viscous folding of magmatic sheets that do not show sub-solidus deformation at grain scale (Fig. 3f). Here, the magmatic foliation dips steeply to nearly vertical (60°-80°) to the east and southeast (dip direction 102°-120°; Fig. 4, b zone) or even locally to the west (dip direction 265–270°).

The silicic unit (Fig. 4, "b" and "c" zones) shows a primarily magmatic foliation. Inside the Quimilo subunit, the alignment of K-feldspar and enclaves defines the fabric development (Fig. 3e). In this subunit, the magmatic foliation is N– S striking and steeply dipping (60°–85°) to the east. The magmatic foliation in the San Agustin subunit displays a regular steeply dipping to the east position (i.e., 60–100°/80° dip direction and dip, respectively). Within the Cerro Blanco subunit, the magmatic foliation is uniformly N– S striking and steeply dipping to the east 60–100°/75–89° (Fig. 4, "c" zone).

Fig. 4 shows interpretative magmatic foliation trending lines based on structural measurements throughout the VFLH batholith. It is important to note that, from outcrop to map scale, magmatic foliations cross over and transpose the gradational contacts among lithologic units.

Within the batholith, there are shear zones that are traceable along hundreds of meters long but less than 2 m thick. This tectonic reworking along narrow and discrete zones transformed plutonic rocks into protomylonite and mylonites. The occurrence of mylonitic zones progressively increases westwards and is dominant adjacent to the western shear zone. However, tectonic structural features will not be considered further for two reasons that are (1) tectonic reworking is always local and subordinate to magmatic foliation, and (2) the study strongly focuses on the magmatic stage of the batholith.

5. Whole rock and mineral geochemistry

The new geochemical data consists of 61 samples with whole rock chemistry plus 21 samples with mineral composition measurement. The full set of new whole rock chemistry and representative mineral composition are given in Appendix A. The location of analyzed samples is shown in the geological map (Fig. 2).

5.1. Whole rock geochemistry

In general, VFLH batholithic rocks are calc-alkalic and magnesian; all but the most SiO_2-rich rocks are metaluminous, however, the alumina saturation index is < 1.1 in the weakly peraluminous granites (Fig. 5a). Plutonic rocks in the typical intermediate subunit (excluding gabbroic rocks) have SiO_2 content ranging from 57 to 71 wt %. Plutonic rocks in the transitional intermediate subunit coincide in the % SiO_2 range with those of the typical intermediate subunit but extend to high values of up to 75 wt %. The SiO_2 contents of rock in the silicic unit largely overlap with the SiO_2 content in the transitional intermediate subunit (62–77 wt %). Considered together, the plutonic rocks spread over a full spectrum of SiO_2 but with two compositional gaps in the ranges 52–57 wt % and 70–73 wt % (Fig. 5b). Irrespective of the host plutonic rocks, magmatic enclaves correspond to the SiO_2 range between 47 and 62 wt %.

The plutonic rocks define a sub-alkaline suite with most of them falling in the mid-K field of the K_2O *vs.* SiO_2 diagram (Fig. 5c). Most major oxides CaO, MgO, TiO_2, and FeO* decrease over the compositional trend while increasing SiO_2. By contrast, K_2O scatters and increases. Only Na_2O shows a singular behavior with a maximum abundance of 3.6 wt % at SiO_2 contents of about 65 wt % (not shown). In the Mg-number *vs.* SiO_2 diagram, intermediate and silicic plutonic rocks display a scattered trend that remains almost constant at *ca.* 0.40 through a wide SiO_2 range. However, the somehow constant trend has a sharp decrease in Mg# after 72 wt % SiO_2 (Fig. 5d). Moreover, the chemical variation trends cross over the limit between tholeiitic to calc-alkaline fields (Otamendi et al., 2009). Both gabbroic bodies and magmatic enclaves in the intermediate unit are the plutonic rocks with $SiO_2 < 52$ wt % in the VFLH batholith. All these mafic plutonic rocks just differ from equivalent rocks of the mafic unit from sierra Valle Fértil – La Huerta in having slightly higher K_2O contents (Fig. 5c).

5.2. Mineral geochemistry

Amphibole is the dominant ferromagnesian mineral in the intermediate unit and is present in almost all the plutonic rocks. According to the Leake et al. (1997) classification, amphiboles are all calcic ($Ca_B > 1.5$) but with significant variations in their abundances of Si, alkalis in A lattice site and $Mg/(Mg + Fe^{2+})$ ratio. In rocks from both the intermediate and silicic units, most amphiboles are either magnesiohastingsite or tschemarkite (Fig. 6a and b). Magnesiohastingsites have higher (Na + K) in A sites and higher total Si (apfu, atoms per formula unit) than tschemarkite amphiboles. Only magnesiohastingsite amphiboles exhibit an increase in their $Mg/(Mg + Fe^{2+})$ ratios with increasing Si contents (apfu). Amphiboles from the intermediate unit show a wide range of $Mg/(Mg + Fe^{2+})$. Conversely, amphiboles from the transitional and silicic units have a narrow range of $Mg/(Mg + Fe^{2+})$ from 0.47 to 0.65, and hence they are in the middle of the compositional spectrum of amphibole from the intermediate unit. Amphiboles display two regular correlations of compositional parameters, one is negative between total alkalis (Na + K) in A sites and Al in tetrahedral (IV) sites, another is positive between Fe^{3+} and Al^{IV}. Compositional variations reflect that the exchange vectors edenite ($Na + Al^{IV} \leftrightarrow [] + Si$) and tschemarkite ($Fe^{3+} + Al^{IV} \leftrightarrow Mg + Si$) controlled the chemical variations.

Biotites in tonalites from the two intermediate subunits have low $Mg/(Mg + Fe^{2+})$ ratios ranging from 0.61 to 0.42. The total Al content varies over a narrow range (1.2–1.5 apfu). All the biotites are in the annite field of the annite – siderophyllite – phlogopite – eastonite compositional field. Biotite is the most abundant ferromagnesian mineral in granodiorites of the silicic unit. Biotites in silicic rocks have $Mg/(Mg + Fe^{2+})$ variable between 0.63 and 0.48 at nearly constant total Al ranging from 1.23 to 1.57 (Fig. 6c). The Ti content of biotite roughly correlates with rock units as it decreases with increasing SiO_2 and alkalis of the whole rock chemistry.

Plagioclase composition varies over a large range considering all the rocks units. There is a nearly continuous trend of decreasing anorthite mole fraction of plagioclase from tonalites of the intermediate unit to granodiorites of the silicic unit. The chemistry of plagioclases in all rocks spreads over the compositional range from labradorite to andesine (An_{55} to An_{40}). A few highly calcic plagioclases ($An > 60$) occur in tonalites from the intermediate unit. Contrasting with little zoned crystal of intermediate rocks, plagioclases in the granodiorites are strongly zoned and show compositions that fall on well-defined clusters and develop albite-rich rims (Fig. 6d).

Orthopyroxene rarely appears in tonalite of the intermediate unit and is always hypersthene with $Mg/(Mg + Fe^{2+})$ ratio of about 0.58. Epidote and sphene are present in granodiorites and tonalites from transitional and silicic units. Epidote shows a pistacite content ranging between 22 and 29%. Sphene is nearly pure but includes detectable amounts of Al and Fe. Magnetite and ilmenite coexist in rock from the typical intermediate subunit. In contrast, magnetite is the unique oxide composing rocks from the transitional and silicic units. Ilmenite in intermediate plutonic rocks contains a constant hematite mole fraction of about 10% (with Fe^{3+} estimated by stoichiometry). In general, magnetite has low ulvospinel mole percentage < 1.

6. U– Pb zircon dating

Separation, CL imaging, and U– Pb dating of zircons were performed

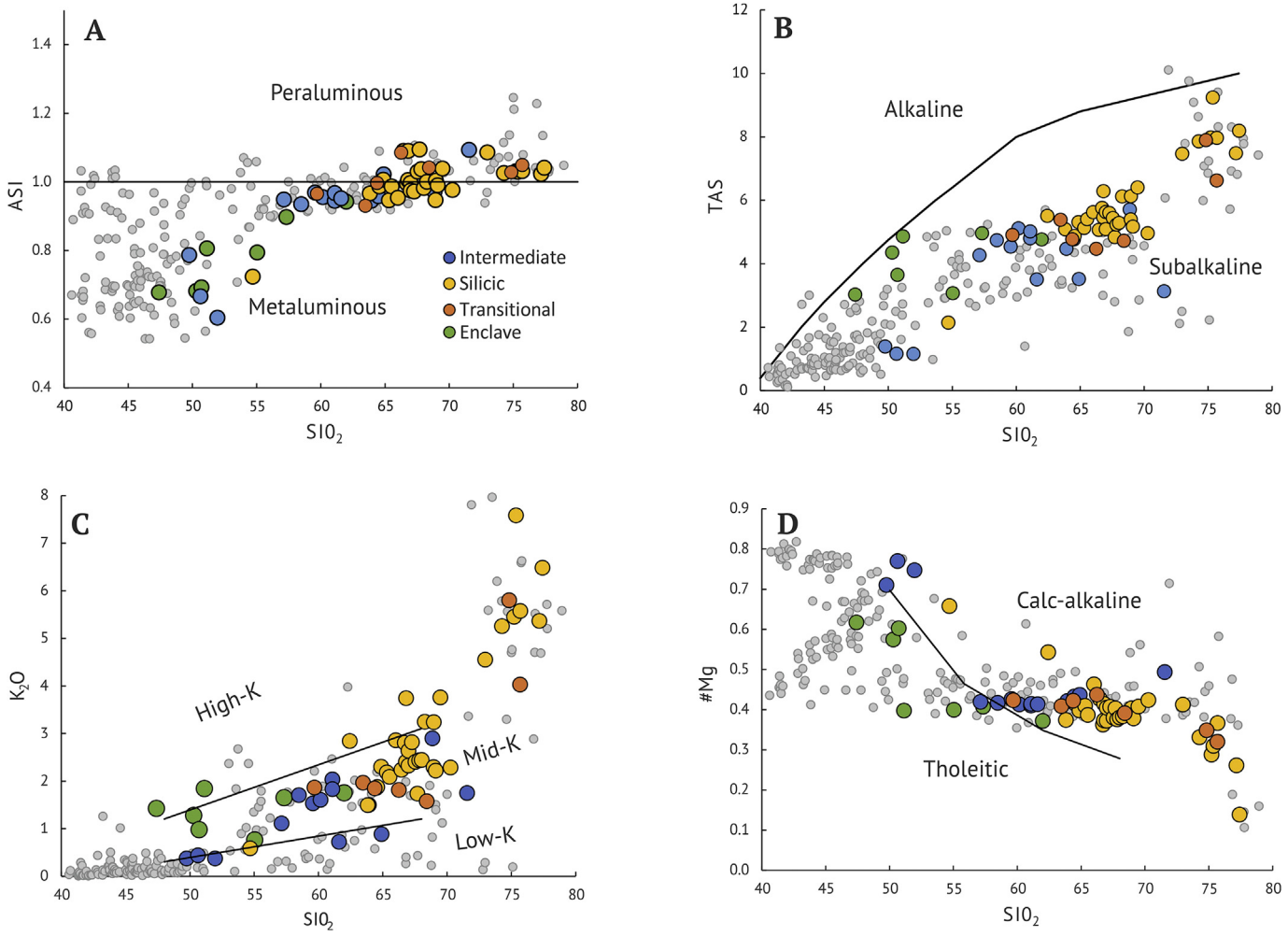

Fig. 5. Harker-type diagrams. (A) Harker–type diagram showing whole rock variation of ASI index ($=Al_2O_3/[CaO + Na_2O + K_2O]$ on a molar basis) against SiO_2. (B) Total alkalis vs. SiO_2 diagram. (C) K_2O vs. SiO_2 diagrams. (B and C) shows the boundaries of igneous series after Le Maitre et al. (1989). (D) Mg-number *vs.* SiO_2 diagram, the line dividing tholeiitic and calc-alkaline fields is after Miyashiro (1974) but converting FeO*/MgO ratio to Mg-number. For comparison with studied rocks, grayed dots project the composition of plutonic rocks from the Sierras de Valle Fértil and La Huerta taken after Otamendi et al. (2012) and Walker et al. (2015).

at the Centro de Excelencia en Geotermia de los Andes (CEGA), Universidad de Chile. Hand-picked zircons were mounted in epoxy resin and later studied using a FEI Quanta 250 scanning electron microscopy. U– Pb dating was performed using a laser ablation system coupled to a iCAP-Q ICPMS. The laser ablation system is an Analyte G2 193 nm ArF excimer laser manufactured by Photon Machines with a double volume HelEx ablation cell that allows ablating in a He environment. To optimize the zircon analysis, the laser was operated at 7 Hz and the ablation diameter used was 30 μm. The Plešovice zircon (Sláma et al., 2008) was used as the primary standard and Sri Lanka-2 (SL-2) (Gehrels et al., 2008) as a secondary standard. Data reduction was carried out using the Iolite software (Paton et al., 2011). Uncertainties are reported at the 2σ level and include measurement internal errors and propagated uncertainties based on the reproducibility of secondary standard (Supplementary data Appendix B).

Three samples from the typical intermediate subunit were analyzed for U– Pb geochronology. The three plutonic rocks contain homogeneous population of zircon grains in terms of shape, size and color. Sample CH10 (bold label in Fig. 2) is a biotite-amphibole-bearing tonalite. Plagioclase occurs as euhedral to subhedral tablets with a homogeneous composition (An_{47}), quartz is interstitial. Intergranular accessory minerals (apatite, ilmenite, magnetite, and zircon) are sparse. Dark-brown biotite is anhedral. Pleochroic dark green to pale-green hornblende is subhedral. Zircons are euhedral or subhedral with prismatic and isometric shapes and vary in size from 50 to 300 μm. Backscatter electron and CL images show the typical compositional zoning (Appendix B). The U content in the analyzed zircons (n = 25) ranges from 540 ppm to 75 ppm, and twenty-two analyses have a Th/U ratio > 0.35 with most Th/U values between 0.40 and 0.55. The best age corresponds to the peak of the Gaussian distribution (Fig. 7a). Twenty-three zircons yielded a weighted mean $^{206}Pb/^{238}U$ age of 475.9 ± 3.2 Ma with an MSWD = 0.51 (Fig. 7b). Two zircons have ages < 465 Ma and are attributed to represent the timing of syn-kinematic metamorphism (e.g., Cristofolini et al., 2014).

Sample CH23 is a tonalite that bears biotite, hornblende and clinopyroxene (for location see Fig. 2 bold label). Uralitized clinopyroxene occurs as small crystals (0.5 mm) remains. Plagioclase is subhedral and without compositional zoning, tends to form bands with hornblende and biotite that are intercalated with quartz-rich bands. Quartz is interstitial. The hornblende is medium grained, euhedral to subhedral. Zircon morphology is simple, the prevalent type is prismatic, isometric and roundly zoned. Nineteen spots were analyzed. The U content is variable (240–1800 ppm). The Th/U ratio values ranging from 0.41 to 0.97. Nineteen zircons yielded a weighted mean $^{206}Pb/^{238}U$ age of 470 ± 5.5 Ma with an MSWD = 1.5. Fig. 7c shows that the best extracted age falls in the maximum peak of the Gaussian curve of the age spectra.

Except for lacking clinopyroxene, sample M20 is a biotite amphibole

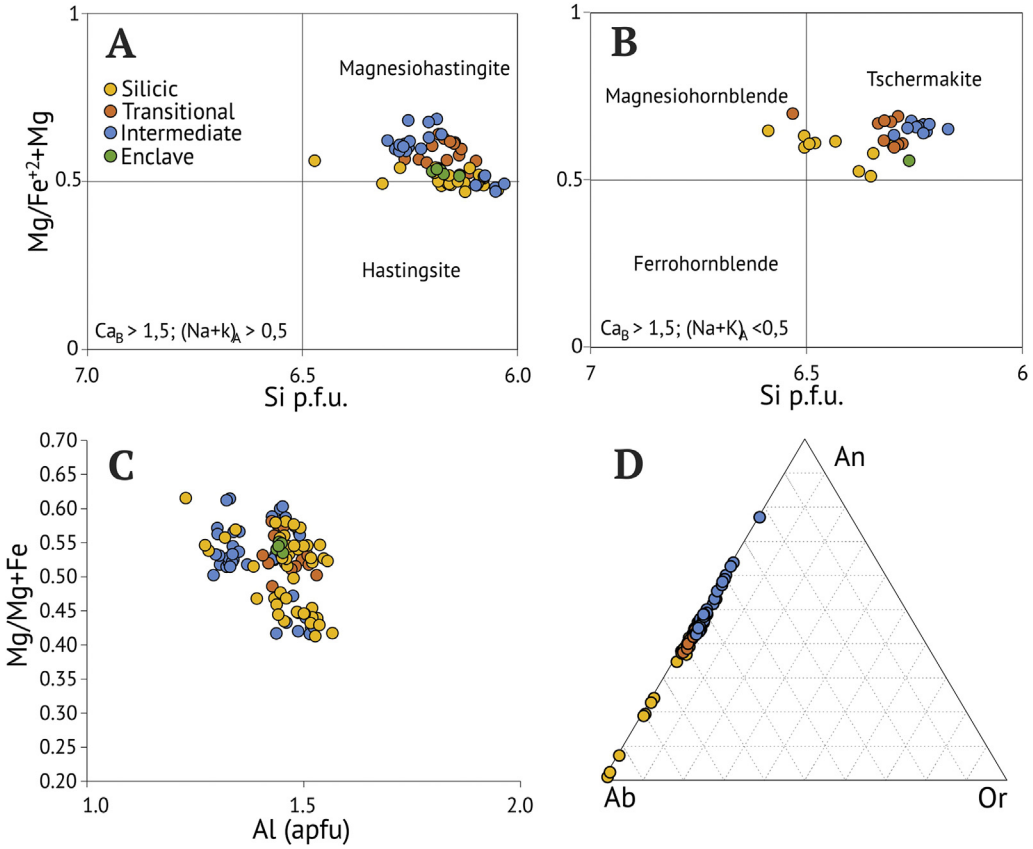

Fig. 6. (A–B) Classification of the calcic amphiboles using the systematic after Leake et al. (1997). (C) Projection of biotite composition in the Mg/(Mg + Fe) *vs.* total Al diagram. (D) Feldspar ternary diagram showing the compositions of plagioclases for different lithologies.

tonalite with a texture and mineralogy very similar to tonalite CH23. Zircons are euhedral to subhedral and prismatic. Backscatter electron images show the typical composition zones. The U content ranges from 104 to 335 ppm. The Th/U ratio varies between 0.5 and 1.37. A weighted mean $^{206}Pb/^{238}U$ age of 465.7 ± 3.6 was obtained from twenty zircons with an MSWD = 0.75. The peak of the Gaussian curve coincides with the best extracted age (Fig. 7e).

Few inherited components were detected in the analyzed zircons. The new ages reported here show that the southern part of sierra Valle Fértil – La Huerta crystallized within the range of published geochronological data for the middle crust of the Famatinian arc (Pankhurst et al., 2000; Ducea et al., 2010, 2017; Castro et al., 2014; Otamendi et al., 2017). The formation of the batholith located from the southern La Huerta to the northern Cerro Blanco (Fig. 2), occurred within a 10 Ma timeframe between 478 and 468 Ma, during the magmatic peak of the Famatinian arc (Ducea et al., 2017; Rapela et al., 2018).

7. P-T estimations

To constrain the position and thickness of the intermediate unit, we determined the equilibrium pressures and temperatures for metasedimentary packages interbedded with the igneous rocks of the intermediate unit. Furthermore, in the discussion section, this study integrates geobarometric results retrieved here with previous paleopressure estimates obtained within all over the extension of the VFLH batholith (Tibaldi et al., 2013, 2011; 2016; Otamendi et al., 2008; Saal, 1993).

The mineral assemblage of Qtz + Pl + Bt + Grt + Sil + Mt/Ilm ± Kfs ± Crd dominating the metasedimentary-derived migmatites found in the VFLH batholith area allows the P-T estimation through more than one geobarometer in each studied rock. Additionally, in the selected metasedimentary migmatites, major minerals combined to perform geobarometry display quite uniform chemistry at sample scale (Appendix C). The mineral composition of the two metasedimentary migmatite specimens (AS30, QLV19) studied here and the methodology used to perform geobarometric estimates are detailed in online Appendix C.

The garnet-bearing metapelite migmatite (AS30) was taken near the boundary between intermediate and silicic units, it occupies an optimal reference for constraining the paleo-depth at which formed the boundary between these two lithostratigraphic units. Equilibrium P-T estimates in sample AS30, using both core and rim compositions yield values ranging from 685 °C to 700 °C and pressures of 5.5 ± 1.1 kbar (GASP), 5.5 ± 1.0 kbar (GBP), 5.4 ± 1.1 kbar (GBQS) and 5.5 ± 1.7 kbar (TH) (Table 1). The agreement of barometric estimates with two thermodynamic models, which are also calibrated using distinct standard state thermodynamic data, heat capacity parameters, and compressibility coefficients, defines a tightly P-T peak condition and locally sets the top of the intermediate unit at a paleopressure of about 5.5 kbar.

The garnet-bearing migmatite QLV19 is located near the exposed core of the intermediate unit. The thermometric calculation using the Fe–Mg exchange vector between garnet and biotite indicates that these rocks equilibrated at 840–850 °C (Berman, 1988). The GASP barometer estimates pressure of 6.8 kbar, whereas GBP barometry yields pressures of 6.5 kbar. Using Thermocalc, multi-reaction equilibria considering the assemblage Grt + Bt + Pl + Qtz ± Sil with and without Crd converge at pressures of 6.3 kbar. Taking all these methods into account suggests equilibration conditions at 840–850 °C and 6.5 ± 0.3 kbar in the migmatites in the core of intermediate unit (Table 1).

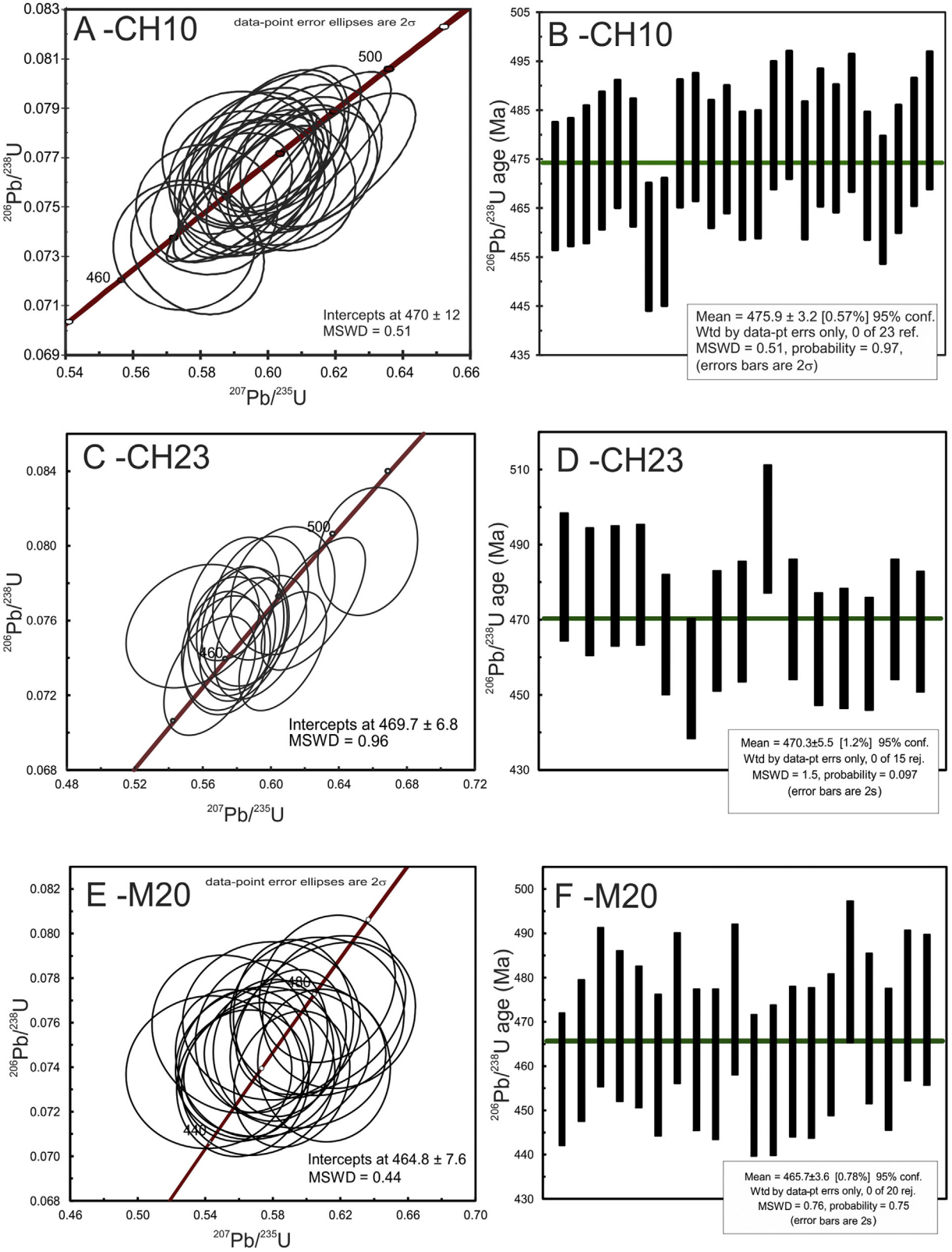

Fig. 7. *In situ* U– Pb zircon ages of a tonalites (CH10, M20 and CH23) in the intermediate unit from the northern region of the La Huerta (Fig. 2 "a" zone). Conventional concordia plot and bars plot displaying spot used to calculate the weighted mean age (A, B) CH10 (C, D) M20 (E, F) CH23.

Table 1
P-T estimations for the metasedimentary rocks.

Sample	Method	T, C°	Method[e]	P, Kbar	Method[e]	P, Kbar	Method[e]	P, Kbar	Method[e]	P, Kbar
QLV19[a]	Gb[c]	840 ± 50	GBQS	6.2 ± 1.35	GASP	6.7 ± 1.3	GBP	6.1 ± 1.0	TH	6.3 ± 0.2
QLV19[b]	Gb[c]	780 ± 50	GBQS	7.6 ± 1.35	GASP	6.5 ± 1.3	GBP	6.8 ± 1.0	TH	6.4 ± 0.2
QLV19[a]	Gb[c]	860 ± 50	GBQS	6.3 ± 1.35	GASP	7.4 ± 1.3	GBP	7.1 ± 1.0	TH	6.0 ± 0.2
QLV19[b]	Gb[c]	760 ± 50	GBQS	4.9 ± 1.35	GASP	5.8 ± 1.3	GBP	5.6 ± 1.0	TH	6.0 ± 0.2
AS30[a]	Gb[d]	690 ± 20	GBQS	5.4 ± 0.6	GASP	5.6 ± 0.5	GBP	5.5 ± 0.5	TH	5.5 ± 0.2
AS30[b]	Gb[d]	670 ± 20	GBQS	6.3 ± 0.6	GASP	5.6 ± 0.5	GBP	5.8 ± 0.5	TH	5.3 ± 0.2
AS30[a]	Gb[d]	645 ± 20	GBQS	5.8 ± 0.6	GASP	5.1 ± 0.6	GBP	5.4 ± 0.5	TH	5.2 ± 0.2
AS30[b]	Gb[d]	660 ± 20	GBQS	6.2 ± 0.6	GASP	4.9 ± 0.6	GBP	5.3 ± 0.5	TH	5.3 ± 0.2

T–P calculations are: (°C ± 1σ) and (kbar ± 1σ) respectively. Ion-exchange and net-transfer reactions with thermometric and barometric properties from Berman (1988) and Berman and Aranovich (1996) are: (GB), Alm + Py = Phl + Ann; (GASP), Grt + Sil + Qtz = Pl; (GBP), (Al2Fe−3/Al2Mg−3) Bt + Grs + Alm/Prp = 3An. When using Berman (1988) and Berman and Aranovich (1996) databases, T and P uncertainties (1σ) are obtained computing more than a dozen of compositional data in every sample.
Thermobarometric estimations using Thermocalc (TH) with (gbps) and (gbpsc) equilibria involving: g, garnet; b, biotite; p, plagioclase; s, sillimanite; c, cordierite.
[a] = Core mineral composition.
[b] = Rim mineral composition.
[c] = T calculation for 7 kbar.
[d] = T calculation for 5 kbar.
[e] = Pressure calculations at T corresponding to GB thermometer.

8. Discussion

8.1. Depth and thickness of the middle crust of the Famatinian arc

The pressures calculated for low variance metapelitic assemblages give better precision and lower uncertainty than those obtained using igneous assemblages (Tibaldi et al., 2011). Metapelitic migmatites and paragneisses occur as discrete screens all over the VFLH batholith and provide P-T estimates that have straightforward interpretations (Fig. 8). Overall, barometric estimates show that the VFLH batholith is exposed from the western boundary with pressures of migmatite crystallization of ≤8 kbar to the eastern covered limit, where pressures are of about 5 kbar. Estimated pressures display a continuous gradient in paleodepths of exposure across the center of sierra Valle Fértil – La Huerta. The few metasedimentary screens in the Cerro Blanco subunit consist of greenschist-facies mineral assemblages, making it difficult to calculate the metamorphic peak pressures for the Cerro Blanco subunit. Regional geology provides evidence for constraining the emplacement pressure of Cerro Blanco subunit. Sierra de Paganzo plutons are at the same latitude but 45 km to the east of Cerro Blanco subunit (Fig. 8). Saal (1993) obtained pressure estimates for the metasedimentary sequence in the Sierra de Paganzo of approximately 3.5 ± 0.5 kbar. This reveals a generalized northward shallower paleodepth of Famatinian arc that culminates in the exposure of the plutonic roof and the supra-batholithic volcano-sedimentary successions in the central Famatina Mountains (Astini and Dávila, 2004; Candiani et al., 2011; Alasino et al., 2016).

The exposure depth of the middle crust of the Early Ordovician Famatinian arc is made by using the P-T data and the computed densities of the plutonic rocks (2.75 g cm^{-3}; Tibaldi et al., 2013). The projection of geobarometric isobars reveals that the deepest parts of the VFLH batholith are at northern and southern extremes of the sierras Valle Fértil - La Huerta (Fig. 8). While, the highest peak metamorphic estimates are on the western boundary of the mafic unit, the basal intermediate plutonic rocks crystallized at paleodepths of about 26 ± 1 km (Tibaldi et al., 2016). Notably, geobarometric estimates suggest that the bottom of the typical intermediate subunit crystallized 3 km shallower in the central sierras Valle Fértil – La Huerta than in the northern and southern extremes of the VFLH batholith (Fig. 8). Considering the northward extension through the Cerro Blanco subunit to the Paganzo batholith, the reconstruction shows that intermediate and silicic rocks dominate the crustal section until a paleodepth lower than 10 km, encompassing more than 15 km of arc crust.

8.2. Reconstruction of uplift and architecture of the middle crust of the Famatinian arc

The data reported in this paper, combined with previous works (Otamendi et al., 2010; Cristofolini et al., 2014; Tibaldi et al., 2013; Castro et al., 2008; Walker et al., 2015; among many others) allowed to reconstruct the magmatic and pos-magmatic history of the VFLH batholith.

The magmatic foliation was developed over the magmatic and submagmatic stages of the plutonic system. Furthermore, the main alignment of elongate mafic microgranular enclaves is parallel to the foliation of the host plutonic rock at all scales. The microgranular enclaves have sharp, crenulated and occasionally diffuse contacts with the host plutonic rock. These relations are attributed to either disaggregation of mafic rocks into evolving intermediate and silicic magma mushes or derived from a hybrid-magma formed as a result of the intrusion of a mafic magma into deep levels of the magmatic system (Webber et al., 2015). In any case, in situ mafic precursors to microgranular enclaves are gabbroic lithologies massively making up the mafic unit (Otamendi et al., 2009).

The presence of quartz filling interstitial space among hornblende and plagioclase grains indicates that quartz crystallized from a residual liquid while the submagmatic deformation was active (Webber et al., 2015). The microstructure hints that the magmatic system responded under a ductile regime whereby a highly viscous magma took up differential stress close to its solidus (Webber et al., 2015). In contrast, deformation over the ductile-brittle transition developed in narrow mylonite belts, occurred when plutonic rocks had completely crystallized (Cristofolini et al., 2014).

The intermediate unit may have remained at magmatic conditions for a few million years, this idea arises from evidence such as: (1) the absence of intrusive contacts among plutonic (sub)units, (2) the development of a penetrative magmatic structure along the entire intermediate unit, and (3) the dated specimens, having almost the same composition, bear zircons crystallized over a time span of ten million years (Fig. 7). The difference in ages is consistent with the sheeted nature of the plutonic lithostratigraphic unit and records the existence of multiple magma batches. In addition, the presence of syn-magmatic mafic intrusions and mafic inclusions, which coexisted with the host plutonic rock in a magmatic state, are observational evidence that the mafic magmatic activity intruded into the intermediate and silicic plutonic system during the few million years that encompassed the construction of the bulk batholith.

Reconstructing the petrological and geochemical evolution of an arc

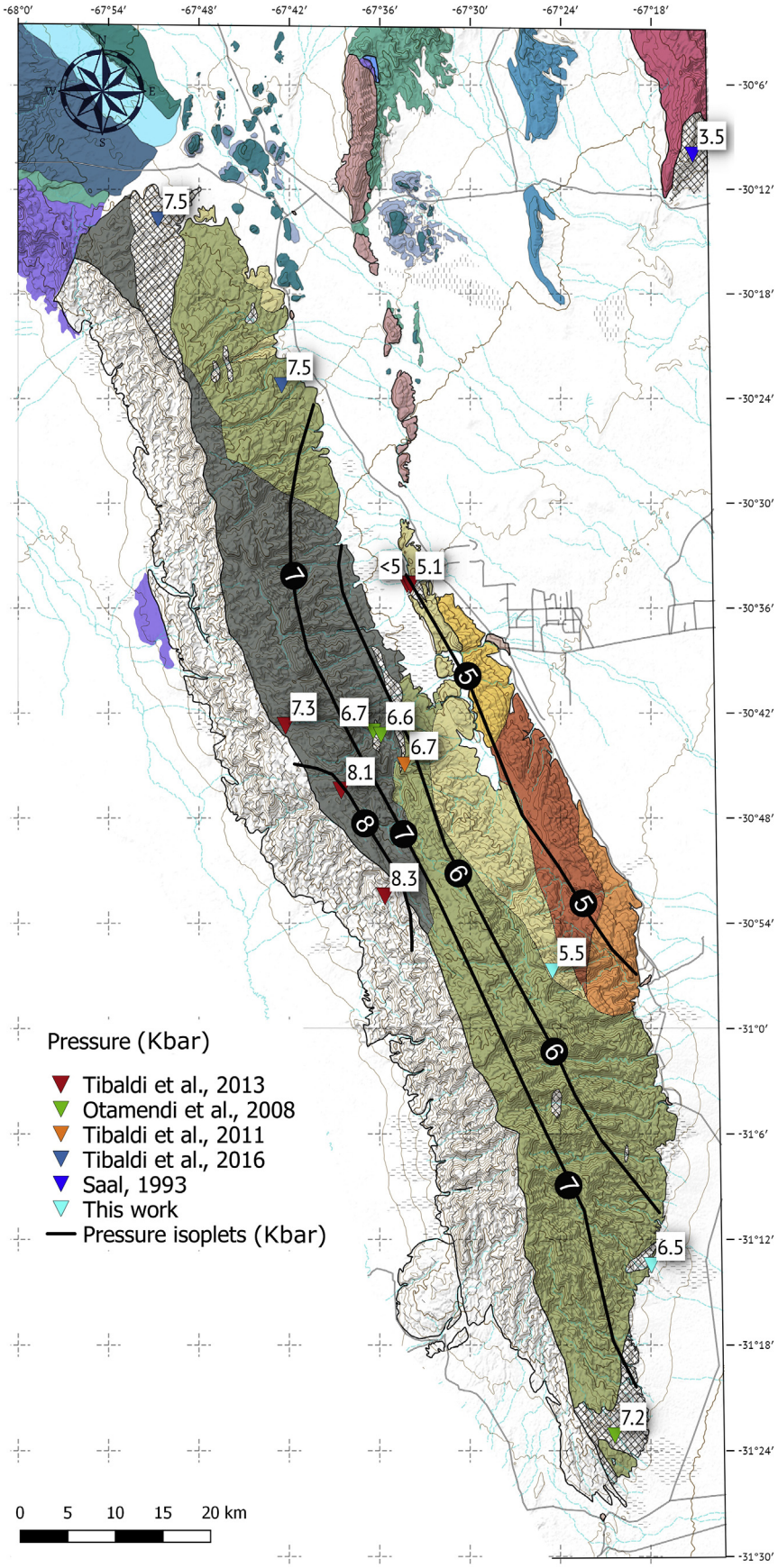

Fig. 8. Map of the VFLH batholith showing calculated pressure in metasedimentary screens. Barometric isopleths for paleodepth of emplacement of the VFLH batholith are compiled from our previous studies and this study.

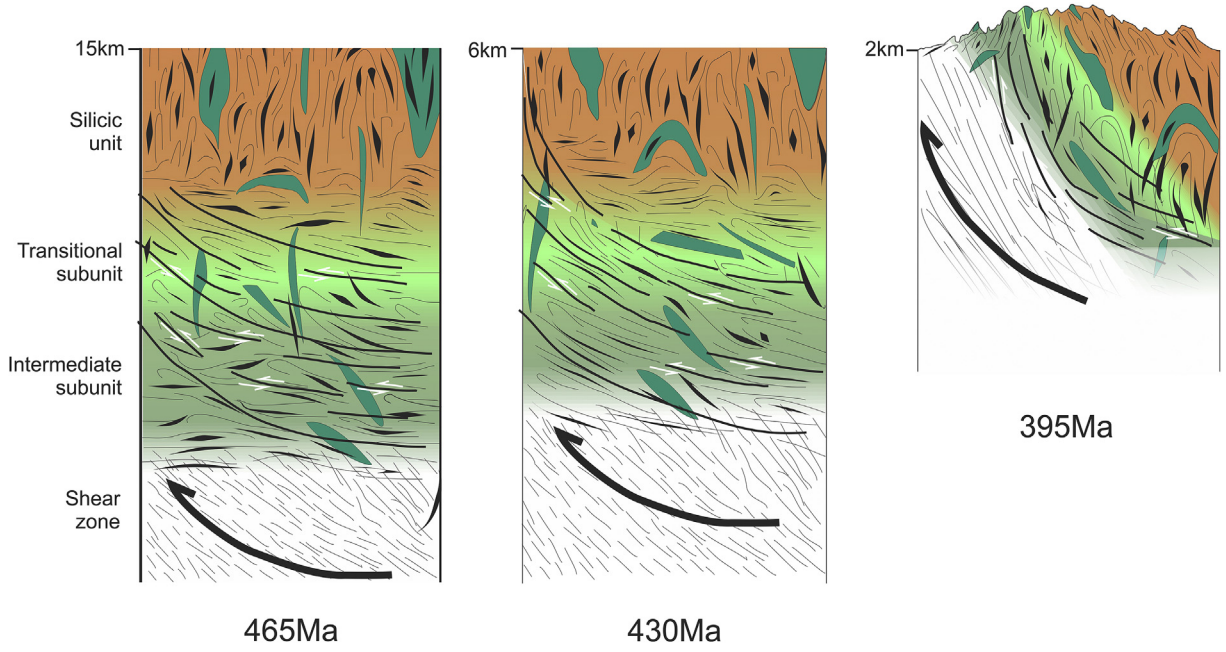

Fig. 9. Schematic structural evolution deduced to explain the deferential uplift in the VFLH batholith. Timing for every stage is taken after Cristofolini et al. (2014). Location of the geological section used to schematize the evolution is shown in Fig. 2.

crustal section requires decoding the pos-magmatic deformational history. There are two robust observations to estimate the degree to which plutonic magmatic structures has tilted, these are: (1) gravity-driven magmatic layering in mafic and ultramafic cumulate (Otamendi et al., 2010) and (2) gravity-driven collapse of magmatic enclaves (Castro et al., 2008). These observations show that the base of the typical intermediate subunit, which is next to the layered cumulates, has been tilted > 70° to the east; whereas the silicic unit in San Agustin (see "b" zone in Figs. 2 and 4) suffered 15-km of unroofing with locally minor tilting (Fig. 9, see Fig. 2 for location of this section). Mainly, large-scale tilting took up in multiple shear zones, the record of which is prominent along the western border of the sierras (Cristofolini et al., 2014). Within the "a" and "b" zones in Fig. 2, local-scale tilting occurs inside the intermediate unit, and it requires to be constrained for restoring the original plutonic crust.

As recovered by pressure estimates from up to 7.4 to < 5.5 kbar, the original thickness of the intermediate unit was about 8 km of arc crust (Fig. 9). However, as exposed today, the intermediate plutonic section varies from > 18-km-wide in the south (Fig. 2, "a" zone) to 5-km-wide in central sierras Valle Fértil – La Huerta (Fig. 2, "b" zone). This raises the question of whether the intermediate plutonic crust is either thickened, or thinned, or had an originally variable thickness. Regardless of alternative explanations, the first conclusion is that the VFLH batholith is not tilted as a single block. Fig. 9 shows an uplift proposal for one example of the rotation of a section that comprehends all igneous units previously described. This idea of rotation could have happened in different degrees and intensities all along the batholith, but our view only assesses the southern section of the batholith (Fig. 2 shows the location of the section).

The intermediate unit is transected by numerous discontinuous shear zones, which are penetrative in plutonic rocks as well as in metasedimentary screens interspersed in the magmatic sequence (Tibaldi et al., 2016). This ductile shear system in the intermediate unit took up strain within a thrusting zone and caused the offset of the magmatic foliation inside the VFLH batholith (Cristofolini et al., 2014). While the plutonic arc sequence was thrusting in the hanging wall of a continent-arc collision, the intermediate unit was uplifted and tilted more than the silicic unit (Fig. 9). During this event, an episode of horizontal shortening of the whole area occurred, associated with vertical stretching, which rotated both lithological contacts and magmatic foliation. The difference in paleo-pressures reflects that the intermediate unit ascended at least 8 km more than the silicic unit. Moreover, westward thrusting decoupled uplifting and eastward tilting must be accounted for restoring the middle arc crust of the Famatinian arc (Fig. 9).

Triassic basaltic floods unconformably overlying all the Ordovician plutonic units (Mirré, 1976; Otamendi et al., 2009) indicate that the low crust of the Famatinian arc was exposed, structured and eroded by the late Paleozoic (Castro de Machuca et al., 2007; Cristofolini et al., 2014). Since the collisional closure of the Ordovician arc to the present, the tectonic reworking of the plutonic sequences was accommodated along narrow ductile shearing and local brittle faults (Figs. 1 and 2). Significantly, an outcome from this work is that, except for the western shear zone, all the plutonic arc crust shows the magmatic structure related to the arc stage.

8.3. Petrogenetic models for the middle crust of the Famatinian arc

In order to test which is the main geologic process that links the different rocks forming the Valle Fértil – La Huerta batholith, we performed straight-forward fractional-crystallization modeling. In the model presented here, major element variations are modeled by stepwise subtraction of minerals that are in the plutonic rocks which are analyzed through electron microprobe, instead of geochemical modeling that needs somehow arbitrarily chosen mineral-melt partition coefficients (Rollinson, 2014). This fractionation model has the advantage that is entirely constrained by field observations, petrographic analyses and compositions of rocks and minerals. The model assumes mass balance whereby the parental melt, the fractionated crystals and the derivative melts are related by a multiple least-squares regression (Rollinson, 2014; Wright, 1974), the methodology and the model are given in online Appendix A. The model sought to replicate both the evolving composition of plutonic rocks and the exposed volume of rock types. Moreover, the crystallization-fractionation model is refined using experimental results and natural examples (Ducea, 2001; Müntener et al., 2001; Jagoutz, 2010; Nandedkar et al., 2014; Paterson and Ducea, 2015; Jagoutz and Klein, 2018; Müntener and Ulmer, 2018; among many others).

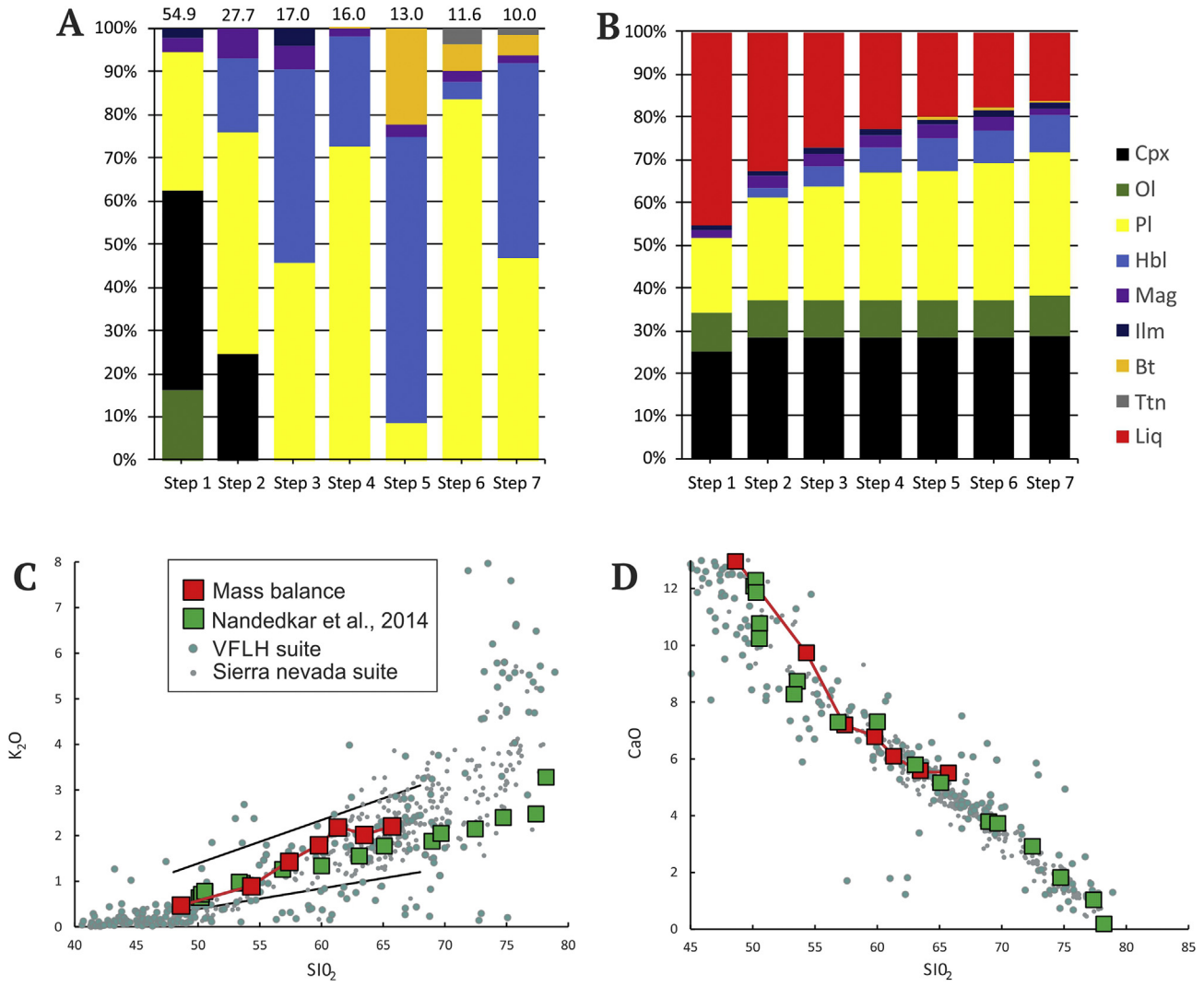

Fig. 10. (A) Mass-balance calculated modal fraction (normalized to 100% weight) of solid phases in simulations of step-wise crystallization-fractionation process linking the studied plutonic rocks. Labels on the right side indicate the color used for each mineral. Labels on the top indicate the absolute fraction (wt%) of solids crystallized in each step of the model. (B) Same as panel (A) but including the modal fraction of liquid (red bar on top) that remains after extracting the accumulated minerals. Total solid composition summarizing the modal proportions of solid phases accumulated relative to the initial gabbroic parental liquid (i.e., specimen LHBL22 in Otamendi et al., 2009). (C) and (D) K_2O vs. SiO_2 and CaO vs. SiO_2 respectively, shows a comparison between the results of mass-balance, the experiment of Nandedkar et al. (2014), the VFLH batholith, and the Sierra Nevada plutonic suite. (For interpretation of the references to color in this figure legend, the reader is referred to the Web version of this article.)

Fig. 10 illustrates the fractionated assemblage providing a summary of the mineral subtraction rescaled to 100% and depicts the mineral phases and their modal proportions crystallizing in every fractionation step. Using a gabbroic composition (LHBL22 in Otamendi et al., 2009) as parental magma, the subtraction of about 25 wt % clinopyroxene, 9 wt % olivine, 18 wt % plagioclase (An_{85}), and 3 wt % Fe– Ti oxides produces a liquid composition closely resembling a diorite with 54% SiO_2. The removal of the cumulate mineral assemblage increases the SiO_2 and reduces the Mg-number of derivative rocks and rationalizes the transition from mafic to intermediate plutonic rocks. Step 2 is olivine-absent and still crystallizes clinopyroxene (7 wt %) while the amount of plagioclase (14 wt %) decreases relative to step 1. Step 3 is clinopyroxene-absent and results in a hornblende gabbroic cumulate of 46 wt % hornblende and 44 wt % plagioclase. In step 4, biotite joins the crystallizing sequence but still amphibole and plagioclase dominate the crystallizing assemblage. Sphene is needed to balance masses at step 7 suggesting it adds as an accessory phase to the crystallizing mineral assemblage.

As the calculated model fits the actual compositions during parent-daughter least squares modeling, a nearly closed-system liquid line of descent theoretically links the plutonic sequence of the intermediate unit. During the first two steps of the fractionation-crystallization model, clinopyroxene and plagioclase are the dominant crystallizing phases that make up more than 80 wt % of cumulate. However, olivine plays an important role in reducing the Mg number. This result is consistent with fractional crystallization experiments (Nandedkar et al., 2014). Crystallization-fractionation modeling by step-wise removal predicts the same proportion of modal plagioclase in the mafic rocks (50%) as measured in experiments of hydrous mafic melts (Müntener et al., 2001; Nandedkar et al., 2014; Müntener and Ulmer, 2018). The composition of plagioclase is anorthite-rich An_{85} in mafic cumulates, while largely evolved plagioclase An_{37} is part of the mineral assemblage of granodioritic magmas. This compositional trend of plagioclase closely matches the composition of quenched plagioclases in fractional crystallization experiments (Nandedkar et al., 2014) supporting the realistic outcome of our fractionation-crystallization model. After the differentiation from gabbro to diorite (i.e., step 2), clinopyroxenes and olivine are no longer parts of the main early crystallizing igneous

assemblage, instead amphibole and plagioclase dominate the crystallizing mineral assemblage.

Cumulates obtained in the model replicate well the cumulate rocks in the mafic unit (Fig. 2). Additionally, the mafic unit assembled deeper than the intermediate unit as an expected consequence of density-driven stratification of rocks dominating each lithostratigraphic unit. In this context, the mafic unit was the natural end place of cumulates generated after magma differentiation. Complementarily, within the intermediate unit the tonalites are heterogeneous owing to the variable content of amphibole and plagioclase, the fractionation-crystallization model replicates that. This result is consistent with petrographic and geochemical observations of tonalites and fractional crystallization experiments (Nandedkar et al., 2014; Müntener and Ulmer, 2018).

The stepwise fractionation model replicates the major oxide contents of the plutonic rocks with SiO_2 < 65 wt % and closely resembles experimentally generated fractionation-crystallization liquid trends (Nandedkar et al., 2014; Müntener and Ulmer, 2018). In contrast, after 65 % wt SiO_2 the plutonic rocks of the VFLH batholith undergo a steep rise in K_2O content that cannot be reproduced by mass-balanced models. The granodioritic daughters formed in steps 6 and 7 have K-feldspar, but if K-feldspar is included in the modeling, the model turns to be statistically unacceptable. Fractionation-crystallization mass balances do not account for the occurrence of magma mixing between tonalitic magmas and leucogranitic melts, a process that is widespread in the area (Fig. 3c and d). The input of K_2O needed to produce K-feldspar megacrysts is almost certainly derived from metasedimentary-derived leucogranitic melts. This also explains the composition of plagioclase in the silicic rocks that is poly-modal ($An_{40 \pm 10}$, $An_{20 \pm 5}$ and $An_{10\text{-}5}$) and requires mixing of tonalitic and leucogranitic magmas.

While fractional crystallization can explain much of the observed plutonic variability, the first step considered in modeling is problematic because it predicts a volume of cumulate rocks not exposed in the Famatinian arc crust. Although our model claims that primitive hydrous-mafic melts are parental to the middle-crust of VFLH batholith, it does not imply that an underlying lower crust is formed from chemically homogenous mantle-derived melts (e.g., Jagoutz et al., 2011). Keeping the caveat in mind, mass-balance models of closed-system fractional crystallization derivate intermediate to silicic magmas (SiO_2 ~ 54–66 wt % and Mg/Mg + Fe^{2+} ~ 0.4) after extracting as much cumulate as a roughly 56 wt % of the primitive melt (SiO_2 ~ 49 wt % and Mg/Mg + Fe^{2+} ~ 0.6). Balancing masses through igneous differentiation results in that the Famatinian magmatic system has left behind within the arc roots 1.12 km^3 of mafic-ultramafic cumulate (density 3100 kg/m^3) while generated 1 km^3 of intermediate and silicic plutonic rock with a density of 2750 kg/m^3 (Fig. 11a). This result is consistent with experimentally derived cumulates from wet basalt differentiation at 7 kbar (Müntener and Ulmer, 2018). The bulk ratio between buoyant intermediate and silicic magmas and weighty cumulates allows reasoning that a column of about 22.5 km depth of dense mafic-ultramafic cumulates should underneath a 20-km-thick column of exposed batholith (Fig. 11a). However, an isolate magmatic column that does not incorporate pre-arc crustal material, generates a maximum amount of arc cumulates (Ducea, 2001; Jagoutz, 2010; Nandedkar et al., 2014; Müntener and Ulmer, 2018). Therefore, this is a maximum estimate for the cumulate root of the Famatinian arc since a significant mass fraction of the batholiths is pre-arc metasedimentary material. For instance, if supracrustal metasedimentary material contributed to making one-third of the 20-km-thick batholitic arc crust, the cumulate sequences would reduce to have been 15 km (Fig. 11b).

These findings lead to some important observations. The entire batholith is a magmatic system where the pre-Ordovician crust was extensively processed to generate plutonic sequences at the batholithic scale. Another related outcome from the field-based petrological modeling is that mass-balanced fractional crystallization yields a 1.3:1 ratio of cumulates to derivative (tonalitic and granodioritic) melt (Figs. 10–11). Therefore, the volume of the non-exposed cumulates

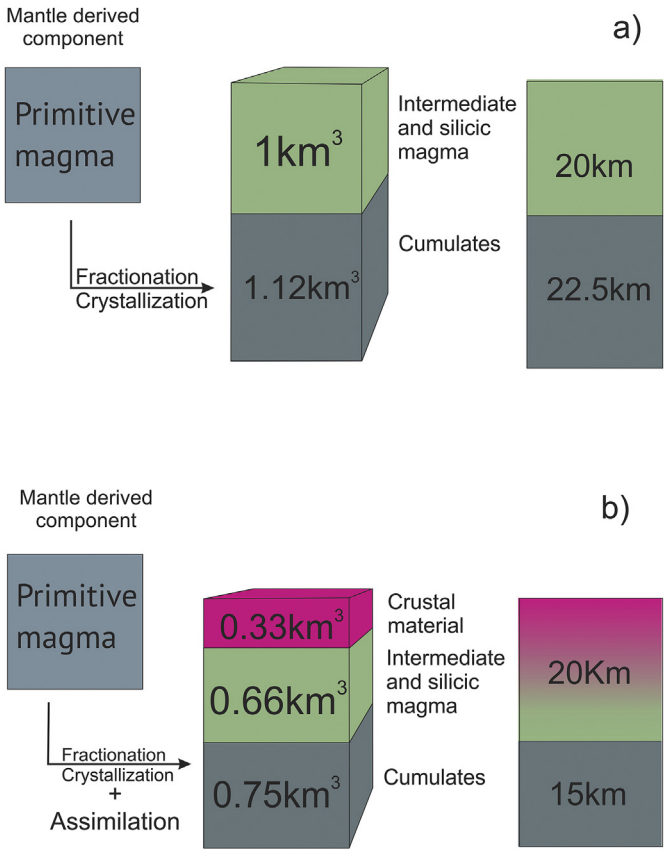

Fig. 11. (A) Cartoon illustration of relative thickness of either cumulates or restites needed to produce 20 km^3 (that is ~middle to upper crust) of intermediate magma, based on stepwise mass-balance calculations. Fractional crystallization requires ~1.3:1 ratio of cumulates to intermediate magmas. (B) Results of calculated ratio of cumulates to intermediate magmas if supracrustal metasedimentary material contributed to make the intermediate magmas.

should be within one to two times thicker than the 20-km-thick intermediate and silicic middle crust. Mantle-derived melts fractioned largely below the seismic Moho then, only the plagioclase-bearing cumulates remaining makes up the arc crust (Saleeby et al., 2003; Jagoutz et al., 2011). However, the assumption of a simple liquid line of descent for a primitive mantle-derived melt that evolved via fractional crystallization may be unlikely. Perhaps, the observation that the arc crust uniquely forms from the differentiation of mantle-derived melts may result in unrealistically high volumes of cumulate ultramafic/mafic sequences. If, as discussed above, a significant component of pre-batholithic metasedimentary masses contributed to the production of intermediate and silicic plutonic rocks, the amount of early-crystallized cumulates, representing complement to tonalites and granodiorites, would be between two-third to one-half lower than the computed estimates through closed-system mass balance. In any case, the Famatinian arc has lost a few tens of kilometers of cogenetic cumulates by either dense root dripping over the magmatic stage or removal during the collisional-related uplift.

8.4. Formation of the middle crust of the Famatinian arc

The construction of an arc crustal section is a spatially and temporally continuous phenomenon that exits among the rather limited observations (Saleeby, 1990, Saleeby et al., 2003). The VFLH batholith assembly took a time period of about 10 Ma and it generated a co-magmatic plutonic crust extending from subvolcanic levels to the low crust (Ducea et al., 2017; Otamendi et al., 2017; Rapela et al., 2018). However, a construction model is separated in stages that only

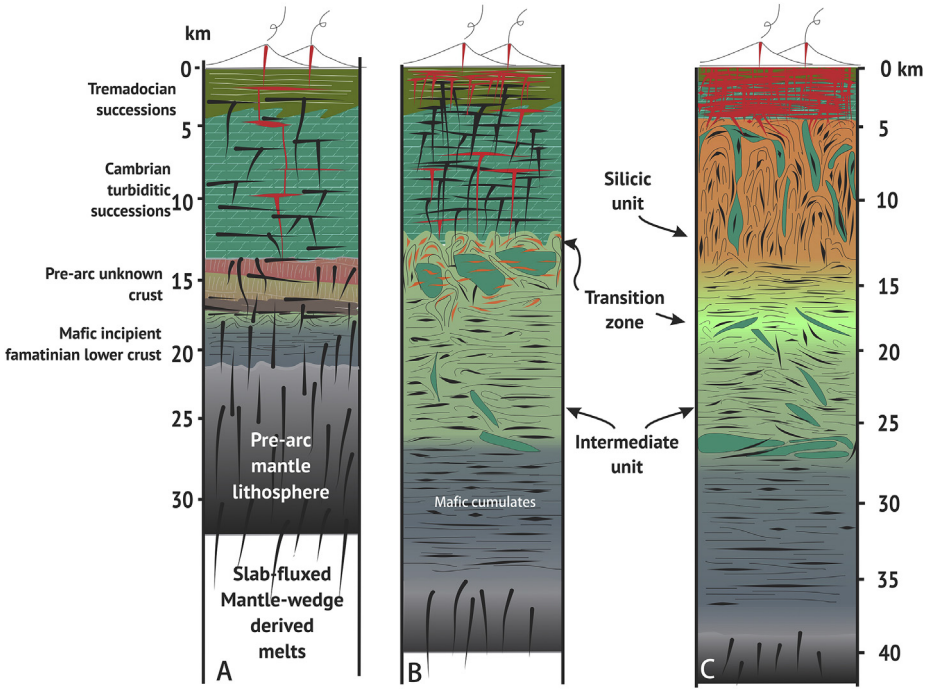

Fig. 12. Schematic working model illustrating the generation of the VFLH batholith within the context of the Famatinian arc. The constructional working model of batholithic crust conserves the main features that were first proposed by Saleeby (1990).

highlight major events (Fig. 12).

Stage 1. Sitting at the top of the mafic lower crust, a 15-km-thick tonalite-dominated batholith is a frozen expression of crustal levels fed by derivate melt that left behind a mafic cumulate sequence (Walker et al., 2015). The process was driven by the emplacement of mafic melts into and onto an externally heated and magmatically evolving lower crust (Annen and Sparks, 2002; Annen et al., 2005). Mafic magmas cooled to the ambient temperature of the "hot zone" and formed cumulate sequences that made up the mafic crust. All the while, their derivative tonalitic differentiates rose upward to build up a mushy middle crust (Bachmann and Bergantz, 2004). As Jagoutz (2010) and Walker et al. (2015) showed, incubation and generation of intermediate melts inside a MASH-like low crustal zone entails a complexity that is, by no means, the simple separation of a parental melt into cumulate sequences and derivative liquids.

Stage 2. Tonalites in the intermediate unit exhibit nearly constant $Mg/Mg + Fe^{2+}$ ratio and aluminosity index with increasing SiO_2 from 55 to 65 wt %. However, the concentration of alkalis, in particular K_2O, shows broad scatter rather than well-defined trends (Fig. 6c). This is related to the generation of distinct batches of tonalitic magmas. While low-K_2O tonalites are magmas derived from closed-system differentiation of primitive mafic melts (Walker et al., 2015), distinctive K_2O-enriched tonalites have a crustal signature imparted on their sources by reaction, mingling, and mixing of mantle and crustal components (Otamendi et al., 2009). The tonalitic middle crust expanded while the geothermal gradient was increasing in the entire arc crust (Annen et al., 2005). At the same time, the tonalitic mushy levels were building up, repetitive entrance and vertical stacking of hydrous mafic magmas into fertile supracrustal successions generated anatectic melt that also drained through the middle intermediate crust (Fig. 12a). This explains why the upper part of the intermediate unit represents major mingling-mixing levels in the batholith formation.

Stage 3. Once the middle crust matured to be a tonalitic-dominated magmatic sequence, it became the structural frame to expand upward constructing the upper silicic zone (Bachmann and Bergantz, 2008; Coint et al., 2013). Granodiorites and granites that made up the silicic upper crust are derivative products of tonalitic mushy magmas that evolved through plagioclase- and amphibole-dominated fractionation, mixing with metasedimentary sourced and anatectic leucogranitic melts (Fig. 12b). A broad compositional overlap among amphibole and plagioclase within intermediate and silicic rock units (Fig. 5) suggests the existence of a large and continuous magmatic system within which differentiation was driven by separation of early crystallized minerals and upward segregation of evolved melt-rich magmas (Coint et al., 2013). This view is also consistent with the trends of magmatic foliations that transect gradational contacts among lithologic units and are mostly parallel to arc strike (Fig. 4). In the silicic unit, particularly along the eastern batholith, the magmatic foliation indicates sub-vertical movement and structural connection over the entire exposed paleo-depths (Fig. 12c). These observations are consistent with magma emplacement by multiple pulses of narrow elongate visco-elastic diapirs within a thermally buffered crustal-wide mushy system (Bachmann and Bergantz, 2008; Miller et al., 2009; Cashman et al., 2017). In contrast, pos-magmatic tectonic reworking and structural tilting within the intermediate unit make it difficult to unravel how assembled the lower levels of the batholith.

Mafic magmas were continuously draining from their mantle sources; they stalled in the low crust and ascended throughout the middle crust (Saal, 1993; Candiani et al., 2011; Otamendi et al., 2012; Alasino et al., 2016). Subduction-related mafic melts carrying dissolved water are capable of ascending throughout the entire crust (Sisson et al., 1996). However, the intermediate to silicic middle crust was a low-density barrier that trapped an undefined fraction of mafic magmatism (Glazner and Ussler, 1988). This is why deformed syn-magmatic mafic dikes and disrupted microgranular mafic inclusions are widely dispersed over the middle crust (Fig. 3). It also reflects that the construction of a middle-crustal arc section and related batholith generation are primarily powered by mantle-derived hydrous mafic magmas (Saleeby et al., 2003; Annen et al., 2005).

9. Conclusions

Results of a field-based geological research supported by petrological, geochemical, and geochronological data show the following

outcomes. (1) Ordovician calc-alkaline plutonic rocks and intervening pre-arc metasedimentary rocks represent a middle-arc crustal section that built up spanning the paleo-depth range from 26 down to < 14 km, making it both the deepest and thickest known exposed batholithic rocks of the Famatinian arc. (2) The VFLH batholith has internal gradational contacts among its lithological units and as a whole expose more than 12 km of paleo-crustal levels. (3) Intermediate calc-alkaline magmas, which crystallize as tonalites at the bottom levels of the batholith, largely differentiate from a complex crystallization-fractionation magmatic system in the lower gabbroic crust. (4) Supracrustally-derived metasedimentary sequences play a major role in fertilizing the magmatic column throughout the entire middle crust, and provide an intracrustal anatectic input required to make up the silicic part of the plutonic batholith.

CRediT authorship contribution statement

Giuliano Camilletti: Conceptualization, Methodology, Formal analysis, Investigation, Writing - original draft, Visualization. **Juan Otamendi:** Conceptualization, Methodology, Funding acquisition, Writing - original draft, Supervision. **Alina Tibaldi:** Conceptualization, Methodology, Writing - review & editing. **Eber Cristofolini:** Methodology, Writing - review & editing. **Mathieu Leisen:** Resources. **Rurik Romero:** Resources. **Fernando Barra:** Resources. **Paula Armas:** Writing - review & editing. **Matías Barzola:** Writing - review & editing.

Acknowledgement

We thank to two anonymous reviewers for their observations, comments and insights that greatly improved this article. We acknowledge financial support from the Argentinean Agencia Nacional de Promoción Científica y Tecnológica, Consejo Nacional de Investigaciones Científicas y Técnicas, and Universidad Nacional de Rio Cuarto. This study was funded by PICT 2014 0958 (FONCYT), grant 2017 Cooperación Internacional Mincyt-CONICET-SNSF, and PPI 2016 18/C485 (Secyt-UNRC). We thank to Asociación Universitaria Iberoamericana de Posgrado (AUIP) for the mobility grant that allowed us to obtain the mineral composition.

References

Alasino, P., Casquet, C., Pankhurst, R., Rapela, C., Dahlquist, J., Galindo, C., Baldo, E., 2016. Mafic rocks of the Ordovician Famatinian magmatic arc (NW Argentina): new insights into the mantle contribution. Geol. Soc. Am 128, 1105–1120 Bulletin.

Annen, C., Sparks, R.S., 2002. Effects of repetitive emplacement of basaltic intrusions on thermal evolution and melt generation in the crust. Earth Planet. Sci. Lett. 203, 937–955.

Annen, C., Blundy, J.D., Sparks, R.S., 2005. The genesis of intermediate and silicic magmas in deep crustal hot zones. J. Petrol. 47, 505–539.

Astini, R.A., Dávila, F.M., 2004. Ordovician back arc foreland and Ocloyic thrust belt development on the western Gondwana margin as a response to Precordillera terrane accretion. Tectonics 23 (4).

Bachmann, O., Bergantz, G.W., 2008. Rhyolites and their source mushes across tectonic settings. J. Petrol. 49, 2277–2285.

Bachmann, O., Bergantz, G.W., 2004. On the origin of crystal-poor rhyolites: extracted from batholithic crystal mushes. J. Petrol. 45 (8), 1565–1582.

Bateman, P.C., Dodge, F.W., 1970. Variations of major chemical constituents across the central Sierra Nevada batholith. Geol. Soc. Am 81, 409–420 Bulletin.

Berman, R.G., 1988. Internally-consistent thermodynamic data for minerals in the system Na2O-K2O-CaO-MgO-FeO-Fe2O3-Al2O3-SiO2-TiO2-H2O-CO2. J. Petrol. 29 (2), 445–522.

Benedetto, J.L., 2004. The allochthony of the Argentine Precordillera ten years later (1993–2003): a new paleobiogeographic test of the microcontinental model. Gondwana Res. 7, 1027–1039.

Berman, R.G., Aranovich, L.Y., 1996. Optimized standard state and solution properties of minerals. Contrib. Mineral. Petrol. 126, 1–24.

Candiani, J., Astini, R., Dávila, F., Collo, G., Ezpeleta, M., Alasino, P., Dahlquist, J., Carrizo, R., 2011. Hojas Geológicas 2969-18, Famatina Y 2969-24, Sañogasta, 1:100.000. Boletín 379. Instituto de Geología y Recursos Minerales, Buenos Aires.

Castro, A., Díaz-Alvarado, J., Fernández, C., 2014. Fractionation and incipient self-granulitization during deep-crust emplacement of Lower Ordovician Valle Fértil batholith at the Gondwana active margin of South America. Gondwana Res. 25, 685–706.

Castro, A., Martino, R., Vujovich, G., Otamendi, J., Pinotti, L., D'Eramo, F., Tibaldi, A., Viñao, A., 2008. Top-down structures of mafic enclaves within the Valle Fértil magmatic complex (early ordovician, san juan, Argentina). Geol. Acta 6, 217–229.

Castro de Machuca, B., Arancibia, G., Morata, D., Belmar, M., Previley, L., Pontoriero, S., 2007. P-T-t evolution of an Early Silurian medium-grade shear zone on the west side of the Famatinian magmatic arc, Argentina: implications for the assembly of the Western Gondwana margin: proterozoic to Mesozoic. Gondwana Res. 13, 216–226.

Cashman, K.V., Sparks, R.S., Blundy, J.D., 2017. Vertically extensive and unstable magmatic systems: a unified view of igneous processes. Science 355 eaag3055.

Cawood, P.A., 2005. Terra australis orogen: rodinia breakup and development of the pacific and iapetus margins of Gondwana during the neoproterozoic and paleozoic. Earth Sci. Rev. 69, 249–279.

Chew, D., Schaltegger, U., Košler, J., Whitehouse, M., Gutjahr, M., Spikings, R., Miškovíc, A., 2007. U-Pb geochronologic evidence for the evolution of the Gondwanan margin of the north-central Andes. Geol. Soc. Am 119, 697–711 Bulletin.

Coint, N., Barnes, C., Yoshinobu, A., Chamberlain, K., Barnes, M., 2013. Batch-wise assembly and zoning of a tilted calc-alkaline batholith: field relations, timing, and compositional variation. Geosphere 9, 1729–1746.

Collins, W.J., 1996. Lachlan Fold Belt granitoids: products of three-component mixing. Earth Environ. Sci. Trans. R. Soc. Edinb. 87, 171–181.

Collo, G., Astini, R., Cawood, P., Buchan, C., Pimentel, M., 2009. U–Pb detrital zircon ages and Sm–Nd isotopic features in low-grade metasedimentary rocks of the Famatina belt: implications for late Neoproterozoic–early Palaeozoic evolution of the proto-Andean margin of Gondwana. J. Geol. Soc. Lond. 166, 303–319.

Creixell, C., Oliveros, V., Vásquez, P., Navarro, J., Vallejos, D., Valin, X., Godoy, E., Ducea, M., 2016. Geodynamics of late carboniferous–early permian forearc in north Chile (28°30′–29°30′S). J. Geol. Soc. 173, 757–772.

Cristofolini, E., Otamendi, J., Ducea, M., Peason, D., Tibaldi, A., Baliani, I., 2012. Detrital zircon U-Pb ages of metasedimentary rocks from the sierra de Valle Fértil: revealing entrapment of late Cambrian marine successions into the deep roots of the early Ordovician Famatinian Arc. J. South Am. Earth Sci. 37, 77–94.

Cristofolini, E., Otamendi, J., Walker Jr., B., Tibaldi, A., Armas, P., Bergantz, G., Martino, R., 2014. A middle paleozoic shear zone in the sierra de Valle Fértil, Argentina: records of a continent-arc collision in the famatinian margin of Gondwana. J. South Am. Earth Sci. 56, 170–185.

Davies, J.H., Stevenson, D.J., 1992. Physical model of source region of subduction zone volcanics. J. Geophys. Res.: Solid Earth 97B2, 2037–2070.

De Bari, S.M., 1997. Evolution of magmas in continental and oceanic arcs: the role of the lower crust. Can. Mineral. 35, 501–519.

Ducea, M., 2001. The California arc: thick granitic batholiths, eclogitic residues, lithospheric-scale thrusting, and magmatic flare-ups. GSA Today (Geol. Soc. Am.) 11 (11), 4–10.

Ducea, M., Otamendi, J., Bergantz, G., Stair, K., Valencia, V., Gehrels, G., 2010. Timing constraints on building an intermediate plutonic arc crustal section: U-Pb zircon geochronology of the Sierra Valle Fértil, Famatinian Arc, Argentina. Tectonics 29, TC4002. https://doi.org/10.1029/2009TC002615.

Ducea, M., Bergantz, G., Crowley, J., Otamendi, J., 2017. Ultrafast magmatic buildup and diversification to produce continental crust during subduction. Geology 45, 235–238.

Glazner, A.F., Ussler III, W., 1988. Trapping of magma at midcrustal density discontinuities. Geophys. Res. Lett. 15, 673–675.

Gehrels, G., Valencia, V., Ruiz, J., 2008. Enhanced precision, accuracy, efficiency, and spatial resolution of U–Pb ages by laser ablation–multicollector–inductively coupled plasma–mass spectrometry. Geochem. Geophys. Geosyst. 9https://doi.org/10.1029/2007GC001805. Q03017.

Jagoutz, O.E., 2010. Construction of the granitoid crust of an island arc. Part II: a quantitative petrogenetic model. Contrib. Mineral. Petrol. 160, 359–381.

Jagoutz, O., Kelemen, P., 2015. Role of arc processes in the formation of continental crust. Annu. Rev. Earth Planet Sci. 43, 363–404.

Jagoutz, O., Klein, B., 2018. On the importance of crystallization-differentiation for the generation of SiO2-rich melts and the compositional build-up of arc (and continental) crust. Am. J. Sci. 318, 29–63.

Jagoutz, O., Müntener, O., Schmidt, M., Burg, J., 2011. The roles of flux-and decompression melting and their respective fractionation lines for continental crust formation: evidence from the Kohistan arc. Earth Planet. Sci. Lett. 303, 25–36.

Jordan, T.E., Allmendinger, R.W., 1986. The Sierras Pampeanas of Argentina; a modern analogue of Rocky Mountain foreland deformation. Am. J. Sci. 286, 737–764.

Leake, B., Woolley, A., Arps, C., Birch, W., Gilbert, M., Grice, J., Hawthorne, F., Kato, A., Kisch, H., Krivovichev, V., Linthout, K., 1997. Nomenclature of amphiboles: report of the subcommittee on amphiboles of the international mineralogical association commission on new minerals and mineral names. Mineral. Mag. 61, 295–321.

Le Maitre, R.W., 1989. A Classification of Igneous Rocks and Glossary of Terms: Oxford. Blackwell Scientific Publications, United Kingdom, pp. 193.

McCulloch, M.T., Gamble, J.A., 1991. Geochemical and geodynamical constraints on subduction zone magmatism. Earth Planet. Sci. Lett. 102 (3–4), 358–374.

Miller, R., Paterson, S., Matzel, J., Snoke, A., 2009. Plutonism at different crustal levels: insights from the~ 5–40 km (paleodepth) North Cascades crustal section, Washington. Crustal cross sections from the western North American Cordillera and elsewhere: implications for tectonic and petrologic processes. Geol. Soc. Am. Spec. Pap. 456, 125–149.

Mirré, J.C., 1976. Descripción Geológica de la Hoja 19e, Valle Fértil, Provincias de San Juan y La Rioja. Servicio Geológico Nacional, Boletín 147, 1–70 Buenos Aires.

Miyashiro, A., 1974. Volcanic rock series in island arcs and active continental margins. Am. J. Sci. 274, 321–355.

Mulcahy, S., Roeske, S., McClelland, W., Ellis, J., Jourdan, F., Renne, P., Vujovich, G.I., 2014. Multiple migmatite events and cooling from granulite facies metamorphism within the Famatina arc margin of northwest Argentina. Tectonics 33. https://doi.

org/10.1002/2013TC003398.
Müntener, O., Kelemen, P., Grove, T., 2001. The role of H2O during crystallization of primitive arc magmas under uppermost mantle conditions and genesis of igneous pyroxenites: an experimental study. Contrib. Mineral. Petrol. 141, 643–658.
Müntener, O., Ulmer, P., 2018. Arc crust formation and differentiation constrained by experimental petrology. Am. J. Sci. 318, 64–89.
Nandedkar, R., Ulmer, P., Müntener, O., 2014. Fractional crystallization of primitive, hydrous arc magmas: an experimental study at 0.7 GPa. Contrib. Mineral. Petrol. 167, 1015.
Otamendi, J., Ducea, M., Bergantz, G., 2012. Geological, petrological and geochemical evidence for progressive construction of an arc crustal section, Sierra de Valle Fértil, Famatinian Arc, Argentina. J. Petrol. 53, 761–800.
Otamendi, J., Ducea, M., Cristofolini, E., Tibaldi, A., Camilletti, G., Bergantz, G., 2017. U-Pb ages and Hf isotope compositions of zircons in plutonic rocks from the central Famatinian arc, Argentina. J. South Am. Earth Sci. 76, 412–426.
Otamendi, J., Ducea, M., Tibaldi, A., Bergantz, G., de la Rosa, J., Vujovich, G., 2009. Generation of tonalitic and dioritic magmas by coupled partial melting of gabbroic and metasedimentary rocks within the deep crust of the Famatinian magmatic arc, Argentina. J. Petrol. 50, 841–873.
Otamendi, J., Pinotti, L., Basei, M., Tibaldi, A., 2010. Evaluation of petrogenetic models for intermediate and silicic plutonic rocks from the Sierra de Valle Fértil-La Huerta, Argentina: petrologic constraints on the origin of igneous rocks in the Ordovician Famatinian-Puna paleoarc. J. South Am. Earth Sci. 30, 29–45.
Otamendi, J., Tibaldi, A., Vujovich, G., Viñao, G., 2008. Metamorphic evolution of migmatites from the deep Famatinian arc crust exposed in sierras Valle Fértil–La Huerta, san juan, Argentina. J. South Am. Earth Sci. 25, 313–335.
Paterson, S., Ducea, M., 2015. Arc magmatic tempos: gathering the evidence. Elements 11, 91–98.
Paterson, S., Vernon, R., Tobisch, O., 1989. A review of criteria for the identification of magmatic and tectonic foliations in granitoids. J. Struct. Geol. 11, 349–363.
Paton, C., Hellstrom, J., Paul, B., Woodhead, J., Hergt, J., 2011. Iolite: freeware for the visualisation and processing of mass spectrometric data. J. Anal. Atomic Spectrom. 26, 2508–2518.
Pankhurst, R.J., Rapela, C.W., Saavedra, J., Baldo, E., Dahlquist, J., Pascua, I., Fanning, C.M., 1998. The Famatinian magmatic arc in the central Sierras Pampeanas: an Early to Mid-Ordovician continental arc on the Gondwana margin. Geol. Soc. Lond. Spec. Publ. 142 (1), 343–367.
Pankhurst, R., Rapela, C., Fanning, C.M., 2000. Age and origin of coeval TTG, I- and S-type granites in the Famatinian belt of NW Argentina. Trans. R. Soc. Edinb. Earth Sci. 91, 151–168.
Putirka, K.D., 2017. Down the crater: where magmas are stored and why they erupt. Elements 13, 11–16.
Ramos, V., 2004. Cuyania, an exotic block to Gondwana: review of a historical success and the present problems. Gondwana Res. 7, 1009–1026.
Ramos, V., 2018. The Famatinian orogen along the protomargin of Western Gondwana: evidence for a nearly continuous Ordovician magmatic arc between Venezuela and Argentina. In: The Evolution of the Chilean-Argentinean Andes. Springer, pp. 133–161.
Ramos, V., Cristallini, E., Pérez, D., 2002. The pampean flat-slab of the central Andes. J. South Am. Earth Sci. 15, 59–78.
Rapela, C., Pankhurst, R., Casquet, C., Dahlquist, J., Fanning, C., Baldo, E., Galindo, C., Ramacciotti, C., Verdecchia, S., Murra, J., Basei, M., 2018. A review of the Famatinian Ordovician magmatism in southern South America: evidence of lithosphere reworking and continental subduction in the early proto-Andean margin of Gondwana. Earth Sci. Rev. 187, 259–285.
Ringwood, A.E., 1974. The petrological evolution of island arc systems: twenty-seventh William Smith Lecture. J. Geol. Soc. 130, 183–204.
Rollinson, H.R., 2014. Using Geochemical Data: Evaluation, Presentation, Interpretation. Routledge.
Saal, A., 1993. El basamento cristalino de la sierra de Paganzo, provincial de La Rioja, Argentina. Thesis (unpublished). Universidad de Córdoba, Córdoba 1- 206.
Saleeby, J.B., 1990. Progress in tectonic and petrogenetic studies in an exposed cross-section of young (~ 100 Ma) continental crust, southern Sierra Nevada, California. In: Exposed Cross-Sections of the Continental Crust. Springer, Dordrecht, pp. 137–158.
Saleeby, J., Ducea, M., Clemens-Knott, D., 2003. Production and loss of high-density batholithic root, southern Sierra Nevada, California. Tectonics 22. https://doi.org/10.1029/2002TC001374.
Sisson, T., Grove, T., Coleman, D., 1996. Hornblende gabbro sill complex at Onion Valley, California, and a mixing origin for the Sierra Nevada batholith. Contrib. Mineral. Petrol. 126, 81–108.
Sláma, J., Košler, J., Condon, D., Crowley, J., Gerdes, A., Hanchar, J., Horstwood, M., Morris, G., Nasdala, L., Norberg, N., Schaltegger, U., 2008. Plešovice zircon—a new natural reference material for U–Pb and Hf isotopic microanalysis. Chem. Geol. 249, 1–35.
Tibaldi, A.M., Álvarez-Valero, A.M., Otamendi, J.E., Cristofollini, E.A., 2011. Formation of paired pelitic and gabbroic migmatites: an empirical investigation of the consistency of geothermometers, geobarometers, and pseudosections. Lithos 122 (1–2), 57–75.
Tibaldi, A., Otamendi, J., Cristofolini, E., Baliani, I., Walker Jr., B., Bergantz, G., 2013. Reconstruction of the Early Ordovician Famatinian arc through thermobarometry in lower and middle crustal exposures, Sierra de Valle Fértil, Argentina. Tectonophysics 589, 151–166.
Tibaldi, A., Cristofolini, E., Otamendi, J., Barzola, M., Armas, P., 2016. Petrología, termobarometría y geoquímica de las rocas anatécticas del sector norte de la sierra de Valle Fértil, San Juan: implicancias en la determinación de variaciones laterales en la construcción del arco magmático. Rev. Asoc. Geol. Argent. 73, 195–210.
Thomas, W., Astini, R., 1996. The Argentine precordillera: a traveler from the Ouachita embayment of North American Laurentia. Science 273, 752–757.
Walker Jr., B., Bergantz, G., Otamendi, J., Ducea, M., Cristofolini, E., 2015. A MASH zone revealed: the mafic complex of the Sierra Valle Fértil. J. Petrol. 56, 1863–1896.
Webber, J.R., Klepeis, K.A., Webb, L.E., Cembrano, J., Morata, D., Mora-Klepeis, G., Arancibia, G., 2015. Deformation and magma transport in a crystallizing plutonic complex, Coastal Batholith, central Chile. Geosphere 11 (5), 1401–1426.
Wright, T.L., 1974. Presentation and interpretation of chemical data for igneous rocks. Contrib. Mineral. Petrol. 48 (4), 233–248.
Yáñez, G., Ranero, C., Huene, R., Díaz, J., 2001. Magnetic anomaly interpretation across the southern central Andes (32–34 S): the role of the Juan Fernández Ridge in the late Tertiary evolution of the margin. J. Geophys. Res. Solid Earth 106, 6325–6345.